FINAL TECHNICAL REPORT

DEVELOPMENT PROGRAM ON MAGNETOELASTIC WAVE AMPLIFIER

by

H. MATTHEWS AND D. H. LYONS

OCTOBER 1967

Prepared by

Sperry Rand Research Center
100 North Road
Sudbury, Massachusetts 01776

Prepared for

MASSACHUSETTS INSTITUTE OF TECHNOLOGY
LINCOLN LABORATORY
P. O. BOX 73
LEXINGTON, MASSACHUSETTS 02173

SRRC-CR-67-51
October 1967

FINAL TECHNICAL REPORT

DEVELOPMENT PROGRAM ON MAGNETOELASTIC WAVE AMPLIFIER

BY

H. Matthews and D. H. Lyons

Prepared by
Sperry Rand Research Center
100 North Road
Sudbury, Massachusetts 01776

for
Massachusetts Institute of Technology
Lincoln Laboratory
P. O. Box 73
Lexington, Massachusetts 02173

Under
Prime Contract No. AF19(628)-5167
Purchase Order No. C-450

Period Covered: 30 June 1966 - 30 June 1967

ABSTRACT

A general theory of parametric excitation of spin waves by a traveling phonon in a ferromagnet is presented. The theory yields expressions for the minimum phonon intensity required for excitation of a pair of spin waves. The threshold intensity is a complicated function of magnetic bias, phonon pump frequency and direction, and the frequency and direction of the excited spin waves. For certain cases of practical interest the threshold expressions together with the conservation conditions for parametric amplification are used through a computer program to generate curves of the functional relation between pertinent variables.

Experiments utilizing suitable transducers and ferrimagnetic material are described. These experiments extend observation of the basic phenomena to include phonon pumping by transverse waves. These experiments generated a curve of relative threshold amplitude versus applied magnetic field for a particular material geometry.

An amplifier device, of exploratory nature, was designed and tested. Because this device failed to generate a signal mode it could not be tested for amplification.

TABLE OF CONTENTS

LIST OF ILLUSTRATIONS

LIST OF ILLUSTRATIONS (cont.)

SECTION I

INTRODUCTION

This report summarizes results achieved during a program entitled "Development Program on Magnetoelastic Wave Amplifier" Subcontract No. 340, under Prime Contract No. AF19(628)-5167. The program envisioned two phases: Phase I, a theoretical evaluation of magnetoelastic amplification; and Phase II, construction of an amplifier to operate in C band with bandwidth greater than 10%.

Prior to the start of this program a specific parametric amplifier device utilizing the magnetic and acoustic properties of yttrium iron garnet (YIG) had been studied theoretically,[1] and parametric amplification of signals propagating in a variety of the modes available in suitably shaped samples of YIG had been observed.[2-4] These studies revealed mechanisms capable of providing net gain at room temperature for signal frequencies ranging from L to X band. However, if pump frequency and bias field were fixed to provide gain at some specified signal frequency, gain was obtained over only a very narrow band centered about the specified frequency.

The limited bandwidth of the mechanisms previously studied results, largely, because the pump wave is not a traveling wave. Among the modes that might be employed as a traveling wave pump in a magnetoelastic amplifier, phonon modes are most attractive since these are essentially independent of magnetic bias field except near magnetoelastic crossover. Thus, with a phonon pump, the bias field can be chosen to select the frequency or wave number of spin wave or other modes without affecting the phonon pump. This lends considerable freedom to the choice of frequency, wave number, propagation direction, etc., of signal and idler modes. These considerations governed the decision to develop a magnetoelastic wave amplifier that employs a traveling phonon pump.

The general feasibility of traveling wave phonon pumping of spin waves in suitable magnetoelastic materials had been demonstrated prior

to the start of the present program Matthews and Morgenthaler had observed the loss of energy from pulses of longitudinal phonons traveling in the direction of the magnetic bias field in a sample of gallium substituted YIG magnetized along a ⟨100⟩ direction.[5] They interpreted the energy loss as due to parametric excitation of a pair of spin waves. This interpretation was supported by their calculation of the instability threshold corresponding to the conditions of their experimental observations.

Parametric excitation of spin waves by a phonon can in principle be used to amplify a spin wave signal provided an appropriate idler spin wave exists so that crystal momentum and energy can be conserved. The gain and bandwidth of an amplifier utilizing the process would depend on the length of the interaction region, the input and output transducer efficiencies, mode of operation (cw or pulsed) and other design features. However, unless the amplitude of the phonon displacement exceeds the minimum required for unstable excitation of spin waves no amplification is possible. Hence the first quantity of interest is this threshold for instability.

A major result of the present program is the generalization of prior calculations to obtain the instability threshold for transverse as well as longitudinal phonons and to include the influence of propagation direction relative to bias field direction and to crystal axes. Section II of this report consists of a summary of these calculations and presents the results by curves giving threshold vs signal frequency for various configurations of pump and signal wave vectors.

The theoretical study showed that for YIG the instability threshold for pumping by transverse phonons is less than for longitudinal phonons. An important new result of the development program is experimental observation of transverse phonon pumping of spin waves, and extension of the pumping frequency from 1 GHz to 3 GHz. Section III of this report consists of a summary of this experiment and of an amplifier experiment.

The development work did not produce a magnetoelastic wave amplifier with usable bandwidth. Section IV of this report contains suggestions for further development work.

SECTION II

THEORY OF PARAMETRIC EXCITATION OF SPIN WAVES BY A TRAVELING PHONON PUMP

2.1 Calculation of Pump Threshold

The magnetoelastic energy density which makes possible phonon spin wave conversion is

$$\mathcal{K}^{ME} = b_1 \alpha_1 e_{xx} + b_2 \alpha_1 \alpha_2 e_{xy} + \text{cyclic permutations}, \tag{1}$$

where b_1 and b_2 are the usual magnetoelastic coupling constants, α_i are the direction cosines of the magnetization, and $e_{\mu\nu}$ are the elastic strains. This energy gives rise to an effective magnetic field

$$\underset{\sim}{H}^{ME} = -\nabla_{\underset{\sim}{M}} \mathcal{K}^{ME} \tag{2}$$

which couples to the magnetization in the usual way. Taking the fourier transform of (2) gives the fourier components of this effective field:

$$H^{ME}_{x,\underset{\sim}{k}} = -\frac{2ib_1}{M^2}\int m_{x,\underset{\sim}{k}-\underset{\sim}{k}'}\, k'_x\, R_{x,k'}\, d\underset{\sim}{k}' - \frac{ib_2}{M^2}\sum_{\mu=y,z}\int m_{\mu,\underset{\sim}{k}-\underset{\sim}{k}'}\left[k'_x\, R_{\mu,k'} + k'_\mu\, R_{x,\underset{\sim}{k}'}\right] d\underset{\sim}{k}' \quad , \tag{3}$$

with $H^{ME}_{y,\underset{\sim}{k}}$, $H^{ME}_{z,\underset{\sim}{k}}$ obtained from (3) by cyclic permutation of the xyz subscripts. The quantities $m_{\nu,\underset{\sim}{k}}$ and $R_{\nu,\underset{\sim}{k}}$ are the $\underset{\sim}{k}$ fourier components of the ν^{th} cartesian components of the magnetization and elastic displacement vectors, respectively. Away from the crossover of the phonon and spin wave dispersion relations, we may neglect all elastic displacements except that caused by the phonon pump, so that

$$R_{\upsilon,\underset{\sim}{k}} = P_\upsilon e^{-i\omega_p t}\,\delta(\underset{\sim}{k}-\underset{\sim}{k}_p) + P_\upsilon^* e^{i\omega_p t}\,\delta(\underset{\sim}{k}+\underset{\sim}{k}_p) \qquad (4)$$

for a pump of frequency ω_p traveling along $\underset{\sim}{k}_p$.

The equations of motion for $m_{x,\underset{\sim}{k}}$ and $m_{y,\underset{\sim}{k}}$ may be conveniently written in matrix form:

$$\dot{m}_{\underset{\sim}{k}} = W_{\underset{\sim}{k}} m_{\underset{\sim}{k}} + Be^{-i\omega_p t}\, m_{\underset{\sim}{k}-\underset{\sim}{k}_p} + B^* e^{i\omega_p t}\, m_{\underset{\sim}{k}+\underset{\sim}{k}_p} \qquad (5)$$

where

$$m_{\underset{\sim}{k}} = \begin{pmatrix} m_{x,\underset{\sim}{k}} \\ \\ m_{y,\underset{\sim}{k}} \end{pmatrix} , \qquad (6)$$

and

$$W_k = \begin{pmatrix} \tfrac{1}{2}\sin 2\phi_k\ \Omega_k(1-\sigma_k^2) & -\Omega_k(\cos^2\phi_k + \sigma_k^2 \sin^2\phi_k) \\ \\ \Omega_k(\sin^2\phi_k + \sigma_k^2 \cos^2\phi_k) & -\tfrac{1}{2}\sin 2\phi_k \Omega_k(1-\sigma_k^2) \end{pmatrix} . \qquad (7)$$

The frequency Ω_k in (7) is the $\theta_k=0$ spin wave frequency,

$$\Omega_k = \gamma(H + Dk^2) \quad ; \qquad (8)$$

the angle ϕ_k is the azimuth angle of $\underset{\sim}{k}$; and

$$\sigma_k = \omega_{\underset{\sim}{k}}/\Omega_k \quad , \qquad (9)$$

where $\omega_{\underset{\sim}{k}}$ is the spin wave frequency:

$$\omega_{\underset{\sim}{k}} = \left[\Omega_k(\Omega_k + 4\pi\gamma M \sin^2\theta_k)\right]^{\frac{1}{2}} \quad . \qquad (10)$$

The terms in (5) involving B and B^* arise from the torque produced by the magnetoelastic field which acts on the magnetization. The matrix B is

$$B = \frac{i\gamma}{M} \begin{pmatrix} -b_2(k_{py}P_x + k_{px}P_y) & 2b_1(k_{pz}P_z - k_{py}P_y) \\ -2b_1(k_{pz}P_z - k_{px}P_x) & b_2(k_{py}P_x + k_{px}P_y) \end{pmatrix} . \tag{11}$$

We now transform to spin wave variables $s_{\underset{\sim}{k}}$, where

$$m_{\underset{\sim}{k}} = T_{\underset{\sim}{k}} \begin{pmatrix} s_{-\underset{\sim}{k}} \\ s^*_{\underset{\sim}{k}} \end{pmatrix} , \tag{12}$$

with the matrix (which diagonalizes $W_{\underset{\sim}{k}}$) given by

$$T_{\underset{\sim}{k}} = \frac{M}{2\sqrt{\sigma_k}} \begin{pmatrix} i\sigma_k \sin\phi_k + \cos\phi_k & -i\sigma_k \sin\phi_k + \cos\phi_k \\ -i\sigma_k \cos\phi_k + \sin\phi_k & i\sigma_k \cos\phi_k + \sin\phi_k \end{pmatrix} . \tag{13}$$

The resulting equations of motion are

$$\begin{aligned} \dot{s}_{-\underset{\sim}{k}} = {} & i\omega_{\underset{\sim}{k}} s_{-\underset{\sim}{k}} + \left(T^{-1}_{\underset{\sim}{k}} B T_{\underset{\sim}{k}-\underset{\sim}{k}_p}\right)_{11} e^{-i\omega_p t} s_{-\underset{\sim}{k}+\underset{\sim}{k}_p} \\ & + \left(T^{-1}_{\underset{\sim}{k}} B T_{\underset{\sim}{k}-\underset{\sim}{k}_p}\right)_{12} e^{-i\omega_p t} s^*_{\underset{\sim}{k}-\underset{\sim}{k}_p} \\ & + \left(T^{-1}_{\underset{\sim}{k}} B^* T_{\underset{\sim}{k}+\underset{\sim}{k}_p}\right)_{11} e^{i\omega_p t} s_{-\underset{\sim}{k}-\underset{\sim}{k}_p} \\ & + \left(T^{-1}_{\underset{\sim}{k}} B^* T_{\underset{\sim}{k}+\underset{\sim}{k}_p}\right)_{12} e^{i\omega_p t} s^*_{\underset{\sim}{k}+\underset{\sim}{k}_p} . \end{aligned} \tag{14}$$

We assume now that the pump frequency ω_p is such as to tend to parametrically excite spin waves with wave vector $-\underset{\sim}{k}$ and $\underset{\sim}{k}+\underset{\sim}{k}_p$, i.e.,

$$\omega_p = \omega_{\underset{\sim}{k}} + \omega_{\underset{\sim}{k}+\underset{\sim}{k}_p} \quad .$$

Noting that $s_{\underset{\sim}{k}} \propto e^{i\omega_{\underset{\sim}{k}} t}$ in the absence of the pump, we see that the last term in (14) drives $s_{-\underset{\sim}{k}}$ at its resonance frequency. Retaining this term, therefore, and dropping as inconsequential the other presumably off-resonance pumping terms, and adding loss gives

$$\dot{s}_{-\underset{\sim}{k}} = (i\omega_{\underset{\sim}{k}} - \lambda_k)\, s_{-\underset{\sim}{k}} + \beta e^{i\omega_p t}\, s^*_{\underset{\sim}{k}'} \quad , \qquad (15)$$

where $\underset{\sim}{k}' \equiv \underset{\sim}{k}+\underset{\sim}{k}_p$; β is the "pumping factor" given by

$$\beta = (T^{-1}_{\underset{\sim}{k}}\, B^*\, T_{\underset{\sim}{k}'})_{12} \quad ; \qquad (16)$$

and

$$\lambda_k = \tfrac{1}{2}\gamma\Delta H_{\underset{\sim}{k}} \quad ,$$

where $\Delta H_{\underset{\sim}{k}}$ is the full spin wave linewidth.

Identical arguments as the above lead to the approximate equation of motion for $s^*_{\underset{\sim}{k}'}$:

$$\dot{s}^*_{\underset{\sim}{k}'} = \beta^* e^{-i\omega_p t}\, s_{-\underset{\sim}{k}} - (i\omega_{\underset{\sim}{k}'} + \lambda_{k'})\, s^*_{\underset{\sim}{k}'} \quad . \qquad (17)$$

The coupled equations (15) and (17) are easily solved exactly, by transforming to the spin wave amplitudes $z_{\underset{\sim}{k}}$:

$$s_{\underset{\sim}{k}} = z_{\underset{\sim}{k}} e^{i\omega_k t} \quad .$$

The $z_{\underset{\sim}{k}}$ obey simple linear equations with constant coefficients:

$$\dot{z}_{-\underset{\sim}{k}} = -\lambda_k z_{-\underset{\sim}{k}} + \beta z^*_{\underset{\sim}{k}'} \quad , \tag{18}$$

$$\dot{z}^*_{\underset{\sim}{k}'} = \beta^* z_{-\underset{\sim}{k}} - \lambda_{k'} z^*_{\underset{\sim}{k}'} \quad . \tag{19}$$

The threshold condition for growth,

$$|\beta|^2 = \lambda_k \lambda_{k'} \quad , \tag{20}$$

is then immediately obtained from (18) and (19) by setting $\dot{z}_{\underset{\sim}{k}} = \dot{z}^*_{\underset{\sim}{k}'} = 0$.

We now turn our attention to finding more explicit expressions for β, the "pumping factor". Using Eqs. (16), (11) and (13), and noting that

$$T^{-1}_{\underset{\sim}{k}} = \frac{1}{M\sqrt{\sigma_k}} \begin{pmatrix} \sigma_k \cos\phi_k - i \sin\phi_k & \sigma_k \sin\phi_k + i \cos\phi_k \\ \sigma_k \cos\phi_k + i \sin\phi_k & \sigma_k \sin\phi_k - i \cos\phi_k \end{pmatrix} ,$$

we find that

$$4\sqrt{\sigma_k \sigma_{k'}}\beta = \tag{21}$$

$$2B^*_{11} \left\{ (\sigma_k + \sigma_{k'}) \cos(\phi_k + \phi_{k'}) - i(1 + \sigma_k \sigma_{k'}) \sin(\phi_k + \phi_{k'}) \right\}$$

$$+ (B^*_{21} + B^*_{12}) \left\{ (\sigma_k + \sigma_{k'}) \sin(\phi_k + \phi_{k'}) + i(1 + \sigma_k \sigma_{k'}) \cos(\phi_k + \phi_{k'}) \right\}$$

$$+ (B^*_{21} - B^*_{12}) \left\{ (\sigma_k - \sigma_{k'}) \sin(\phi_k - \phi_{k'}) + i(1 - \sigma_k \sigma_{k'}) \cos(\phi_k - \phi_{k'}) \right\} .$$

For a longitudinal pump of amplitude A,

$$2B^{*}_{11} = A\eta_2 \sin^2\theta_p \sin 2\phi_p \quad , \tag{22}$$

$$B^{*}_{21} + B^{*}_{12} = -A\eta_1 \sin^2\theta_p \cos 2\phi_p \quad , \tag{23}$$

$$B^{*}_{21} - B^{*}_{12} = A\eta_1 (3\cos^2\theta_p - 1) \quad , \tag{24}$$

where

$$\eta_i = i\gamma b_i k_p / M \quad .$$

Matthews and Morgenthaler[5] have calculated the instability threshold for a longitudinal pump traveling along z. For this case,

$\theta_p = 0$, $\phi_{k'} = \phi_k + \pi$, and β becomes

$$\beta = \frac{\gamma A k_p b_1 (1 - \sigma_k \sigma_{k'})}{2M\sqrt{\sigma_k \sigma_{k'}}} \quad .$$

Setting $|\beta'|^2 = \frac{1}{4}\gamma^2 \Delta H_k \Delta H_{k'}$, gives a critical amplitude A in agreement with Eq. (10) of reference (1). A further check on (21) is obtained by considering the case of magnetoelastic isotropy, $b_1 = b_2$. Then β depends on azimuth angles only through the combination $\phi_k + \phi_{k'} - 2\phi_p$, and hence is independent of rotations of the crystal about the z axis.

The case of a transversely polarized pump is slightly more complicated. We assume that the medium is elastically isotropic, an assumption fairly good for YIG. Then the general shear polarization is elliptical and can be characterized by the amplitude A_t of the elastic displacement perpendicular to the wave vector $\underset{\sim}{k}_p$ and in the plane of $\underset{\sim}{k}_p$

and the z axis, by the amplitude A_t, of the elastic displacement perpendicular to this plane, and by the phase difference ψ between these displacements. Thus, we write the elastic displacement vector as

$$\underset{\sim}{R} = A_t \cos(\underset{\sim}{k}_p \cdot \underset{\sim}{r} - \omega_p t)\hat{t} + A_t' \cos(\underset{\sim}{k}_p \cdot \underset{\sim}{r} - \omega_p t - \psi)\hat{t}'$$

where the vectors $\hat{t}$ and $\hat{t}'$ are shown in Fig. 1. Then,

$$2B^*_{11} = \eta_2 \sin\theta_p \left\{ A_t \cos\theta_p \sin 2\phi_p + A_t' e^{i\psi} \cos 2\phi_p \right\} , \quad (25)$$

$$B^*_{21} + B^*_{12} = \eta_1 \sin\theta_p \left\{ A_t \cos\theta_p \cos 2\phi_p - A_t' e^{i\psi} \sin 2\phi_p \right\} , \quad (26)$$

$$B^*_{21} - B^*_{12} = -3\eta_1 \sin\theta_p \cos\theta_p A_t . \quad (27)$$

Equations (20) through (27) constitute a convenient set of formulas to calculate the instability threshold for any pump polarization and wave vector of interest.

In the case of a transverse phonon pump, the threshold power depends on the state of elliptical polarization in a complex way, as can be seen from the above equations. In order to reduce the number of cases to consider, we analyze only what is perhaps the most interesting case, namely the case of optimum polarization. That is, we choose the phase ψ and amplitudes A_t and A_t', that minimize $|\beta|^2$, subject to the constraint that the acoustic intensity

$$I = \tfrac{1}{4} C_{44} k_p^2 v_t \left(A_t^2 + A_t'^2 \right) \quad (28)$$

is constant. In (28), C_{44} is the transverse elastic stiffness, and v_t is the transverse sound velocity. The optimum polarization is easily found analytically, since $|\beta|$ is of the form:

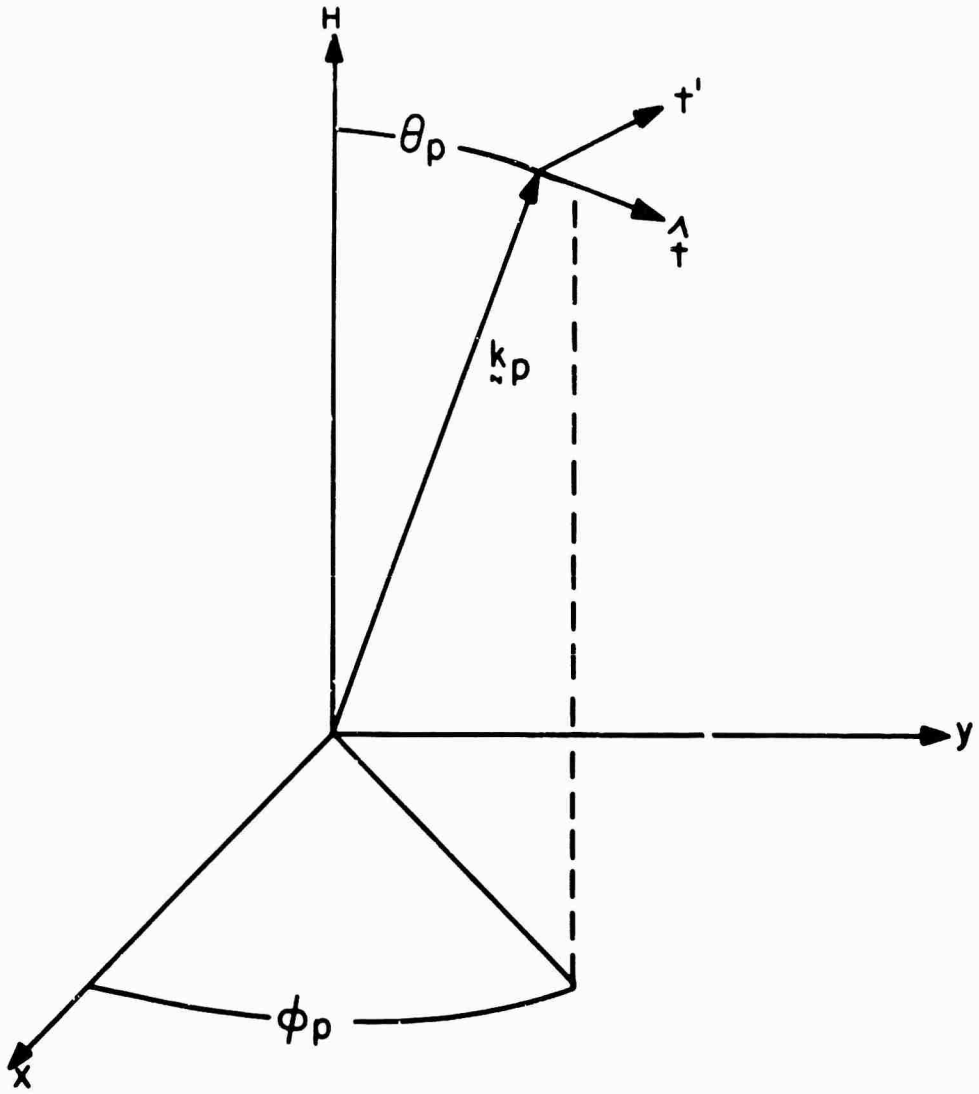

FIG. 1 Coordinate system showing $\hat{t}$ and $\hat{t}'$ directions.

$$|\beta| = |A_t r_t e^{i\psi_t} + A_{t'} r_{t'} e^{i(\psi_{t'}+\psi)}| \quad , \tag{29}$$

where r_t and $r_{t'}$ are the absolute values of the coefficients of A_t and $A_{t'}$, respectively. Clearly,

$$\psi = \psi_t - \psi_{t'} \tag{30}$$

is the optimum phase, so that

$$\max_{\psi} |\beta| = A_t r_t + A_{t'} r_{t'} \quad . \tag{31}$$

The right side of (31) may be considered to be the inner product of the vector $(A_t, A_{t'})$ with the vector $(r_t, r_{t'})$, while the intensity I is proportional to the square of the length of $(A_t, A_{t'})$. Thus, the right side of (31) is clearly maximized, when I is constrained to be constant, by choosing $(A_t, A_{t'})$ parallel to $(r_t, r_{t'})$, that is

$$A_t/A_{t'} = r_t/r_{t'} \quad . \tag{32}$$

Defining, then, $A^2 = A_t^2 + A_{t'}^2$, we have the result

$$\max_{\text{elliptical polarizations}} |\beta| = A\sqrt{r_t^2 + r_{t'}^2} \quad , \tag{33}$$

with the optimum polarization defined by (31) and (33).

Later on, we shall concentrate our attention on the case of $\theta_p = 90^0$. It is clear physically and from Eqs. (25) through (27) that, in this case, the elastic displacement along $\hat{t}$ does not couple to the spin waves ($r_t = 0$). Hence, the instability threshold for the growth of any pair of spin waves is minimized by having the transverse pump linearly

polarized in the $\hat{t}'$ direction (in this case, on the xy plane).

As already mentioned, we have assumed throughout the analysis that the energy and wave vector conservation conditions

$$\omega_{\underset{\sim}{k}} + \omega_{\underset{\sim}{k}'} = \omega_p \quad , \tag{34}$$

$$\underset{\sim}{k} + \underset{\sim}{k}' = \underset{\sim}{k}_p \tag{35}$$

are satisfied. Therefore, before we can apply the formulas derived above, we must consider the general question of satisfying these conditions. This we do in the next section.

2.2 Energy and Wave Vector Conservation

The conservation conditions (34) and (35) plus the dispersion relations

$$\omega_p = v_s k_p \tag{36}$$

$$\omega_{\underset{\sim}{q}} = \gamma\left[(H+Dq^2)(H+Dq^2+4\pi M \sin^{-2}\theta_q)\right]^{1/2} \qquad \underset{\sim}{q} = \underset{\sim}{k},\ \underset{\sim}{k}' \tag{37}$$

constitute a set of seven (scalar) equations in the thirteen variables

$$\omega_p,\ \omega_k,\ \omega_{k'},\ k_p,\ \theta_p,\ \phi_p,\ k,\ \theta_k,\ \phi_k,\ k',\ \theta_{k'},\ \phi_{k'},\ H\ .$$

It is possible, therefore, to fix six of the thirteen variables, and determine the remaining seven from the above conditions.

In accord with practical considerations concerning the realization of a magnetoelastic amplifier utilizing a phonon pump with spin wave signal and idler, we choose to fix the pump variables ω_p, θ_p, ϕ_p, the signal variables ω_k, θ_k and the internal field H. Only for values of these variables within certain limits do real (physical) solutions for

the remaining variables exist. These limits define upper bounds to the bandwidth under various conditions of operation.

The threshold pump power required for gain also depends on the above thirteen quantities in addition to the spin wave linewidths, magnetoelastic coupling constants and pump polarization. Therefore, solving the conservation conditions is a necessary first step in computing the threshold power for gain. We have solved the seven equations above on a computer for various conditions of operation. Typical results are displayed in Figs. 2, 3, 4 and 5.

We note from these figures that solutions exist over large regions of parametric space. For example, in a field of 1000 gauss, a signal propagating at an angle of 45^0 to the field could be amplified, so long as the signal frequency is between 4.5×10^{10} rad/sec and 6.0×10^{10} rad/sec. As the signal frequency changes from the lower to the upper value, the figures show that the azimuthal angle of the signal wave vector must change from $\pm 135^0$ to $\pm 28^0$ (for $\phi_p=0$). The $\pm$ sign comes from the fact that solutions come in pairs since each solution $\underset{\sim}{k}$, $\underset{\sim}{k}'$ can be reflected in the $\underset{\sim}{H}$, $\underset{\sim}{k}_p$ plane to give a second solution to the conservation conditions. In general, for $\phi_p \neq 0$, these two different solutions will have different instability thresholds as a result of the magnetoelastic anisotropy $b_1 \neq b_2$.

The preceding theory may now be applied to the computation of instability thresholds for various configurations of signal and pump wave vectors. We have used the following values,[6,7] appropriate to YIG, in the numerical computations resulting in Figs. 6 through 15:

$$C_{11} = 2.69 \times 10^{12} \text{ d/cm}^2 ,$$

$$C_{44} = 7.64 \times 10^{11} \text{ d/cm}^2 ,$$

$$\rho = 5.17 \text{ gm/cm}^3 ,$$

$$b_1 = 3.48 \times 10^6 \text{ ergs/cm}^3 ,$$

$$b_2 = 6.96 \times 10^6 \text{ ergs/cm}^3 ,$$

$$D = 5.2 \times 10^{-3} \text{ Oe-cm}^2 ,$$

$$4\pi\gamma M = 3.1 \times 10^{10} \text{ sec}^{-1} .$$

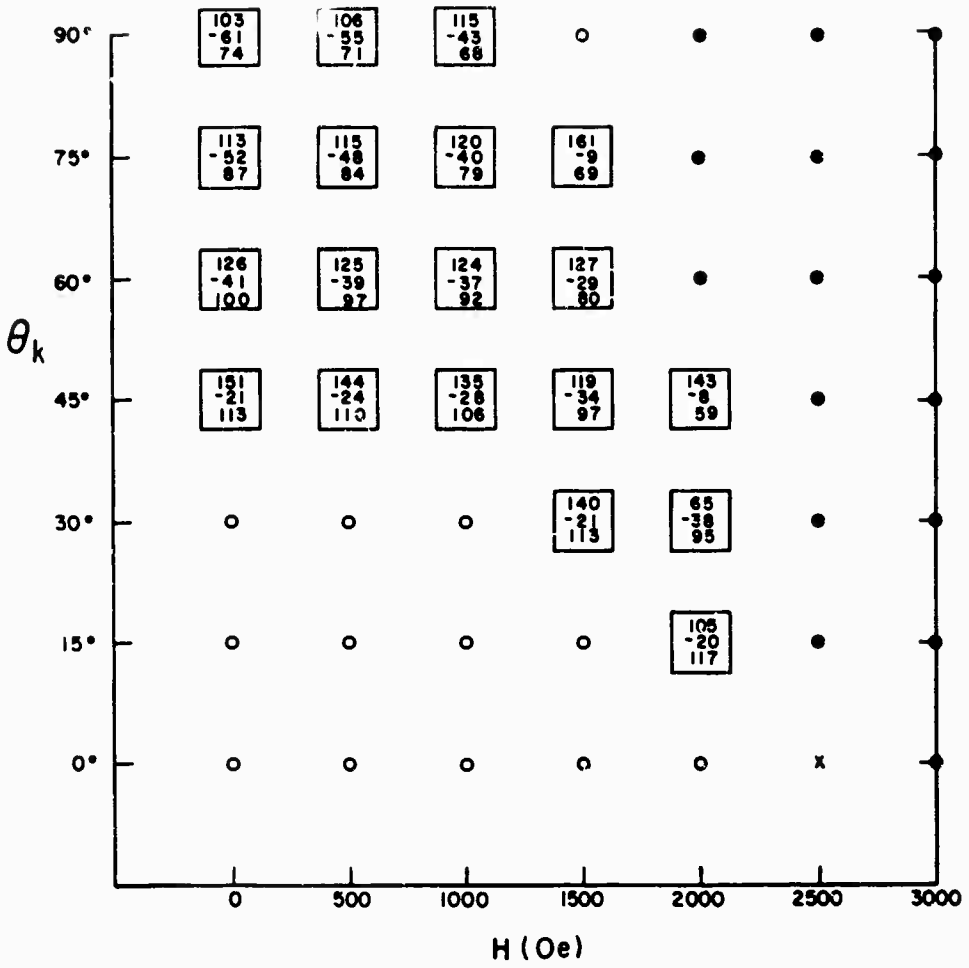

FIG. 2 Solutions to the conservation conditions for a transverse acoustic pump in YIG. The relevant parameters are:

$4\pi\gamma M = 4.2224 \times 10^{10}$ rad/sec $\quad \theta_p = 45^0 \quad \omega_k = 4.5 \times 10^{10}$ rad/sec

$v_s = 3.843 \times 10^5$ cm/sec $\quad \varphi_p = 0^0 \quad \omega_p = 10^{11}$ rad/sec

$D = 5.2 \times 10^{-9}$ gauss cm^2

Real solutions exist for the values of the internal field H and the signal wave vector polar angle θ_k indicated by the boxes. The three numbers in each box are, from top to bottom, the signal wave vector aximuthal angle φ_k, the idler wave vector azimuthal angle $\varphi_{k'}$, and the polar angle $\theta_{k'}$ (all angles in degrees). Symbols where no real solution exists indicate the reason for failure as follows:

- • $\omega_k < \gamma[H(H + 4\pi M \sin^2\theta_k)]^{1/2}$
- * $\omega_{k'} < \gamma H$
- Δ k' less than $k_{pz} - k_z$
- x No triangle can be formed from lengths k, k', k_p
- 0 No triangle can be formed from xy-projections of $\underset{\sim}{k}$, $\underset{\sim}{k'}$, $\underset{\sim}{k}_p$

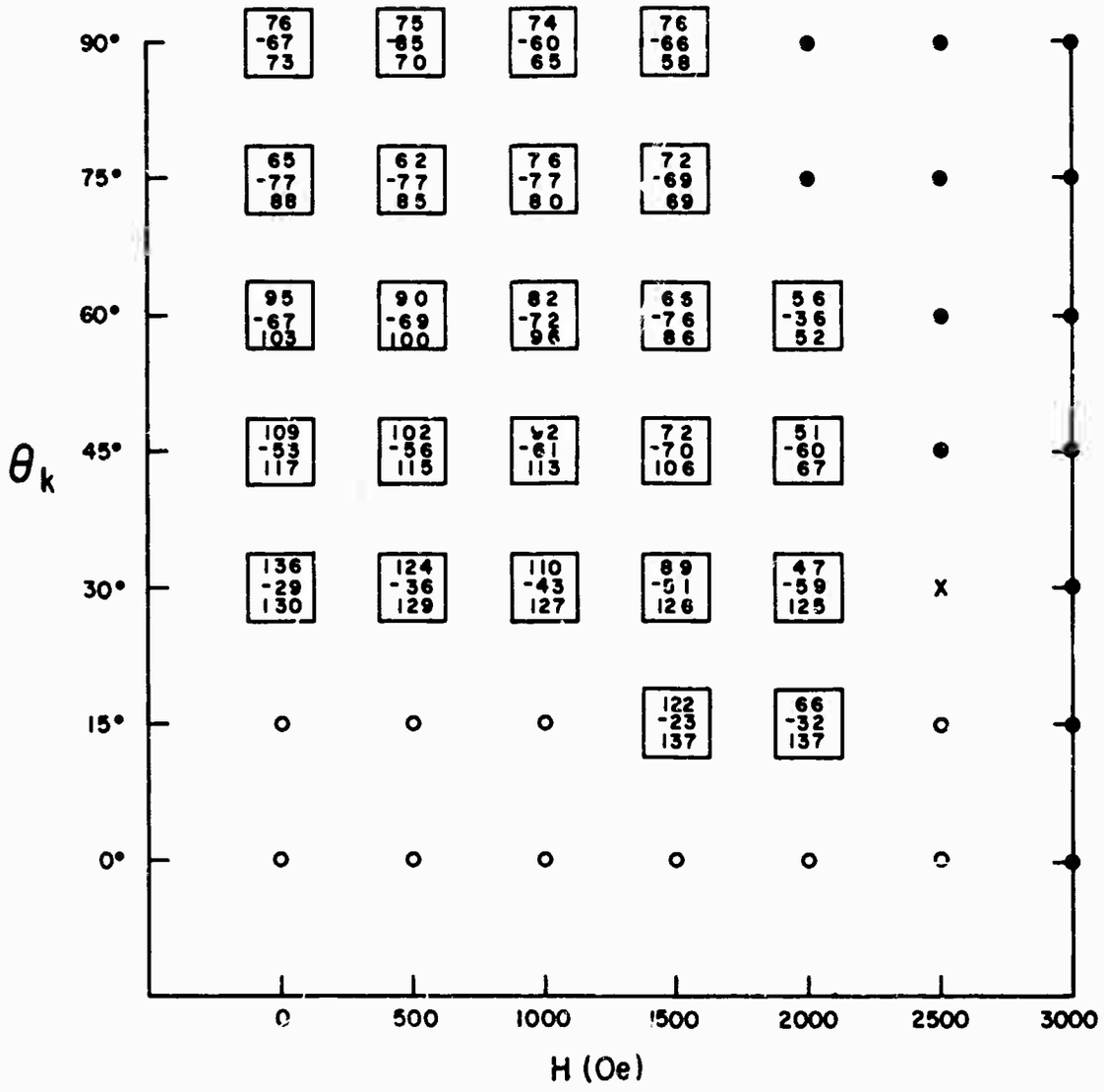

FIG. 3 Same as Fig. 2, except $\omega_k = 5 \times 10^{10}$ rad/sec. This is the degenerate (in frequency) case.

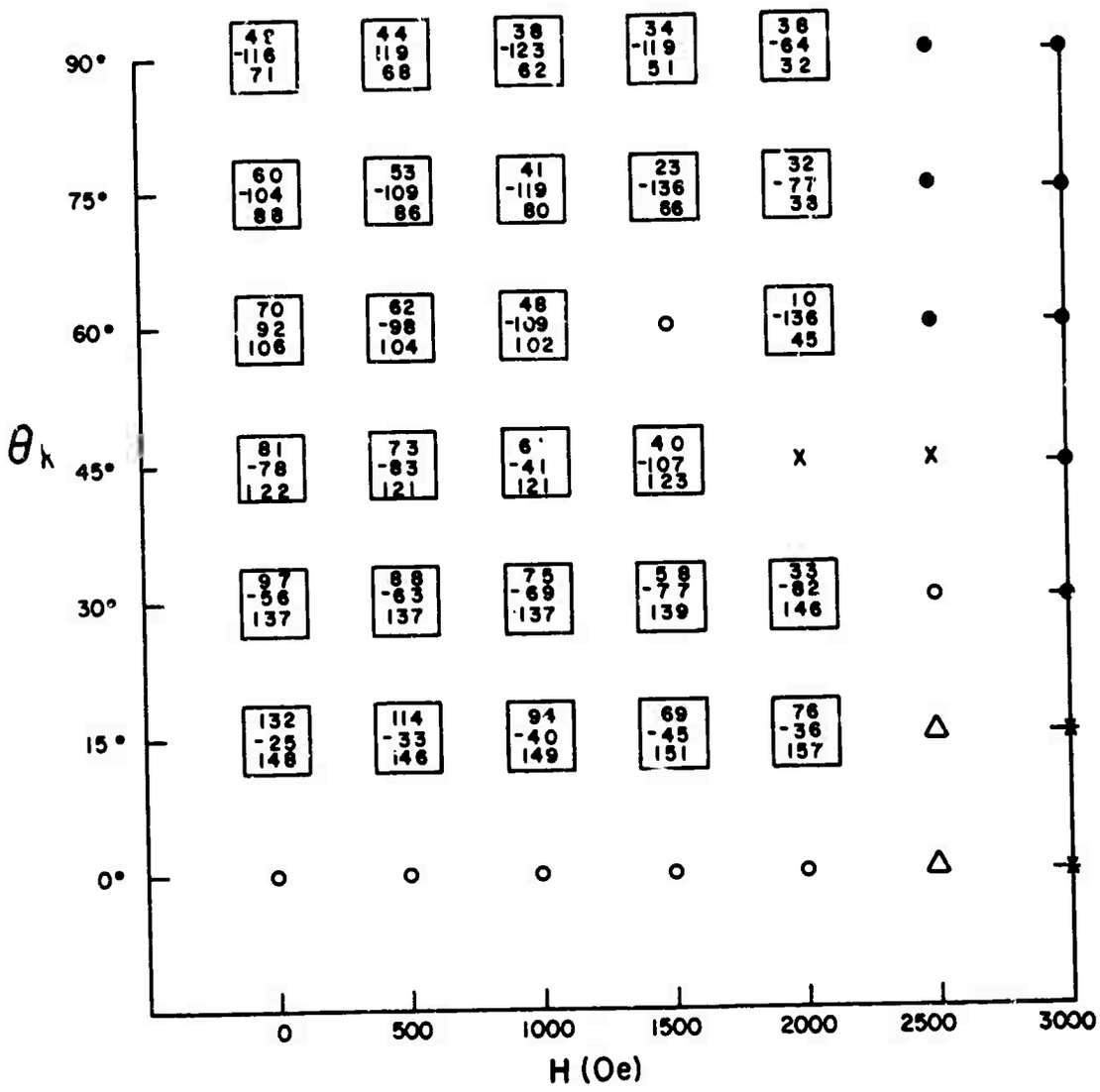

FIG. 4 Same as Fig. 2, except $\omega_k = 5.5 \times 10^{10}$ rad/sec.

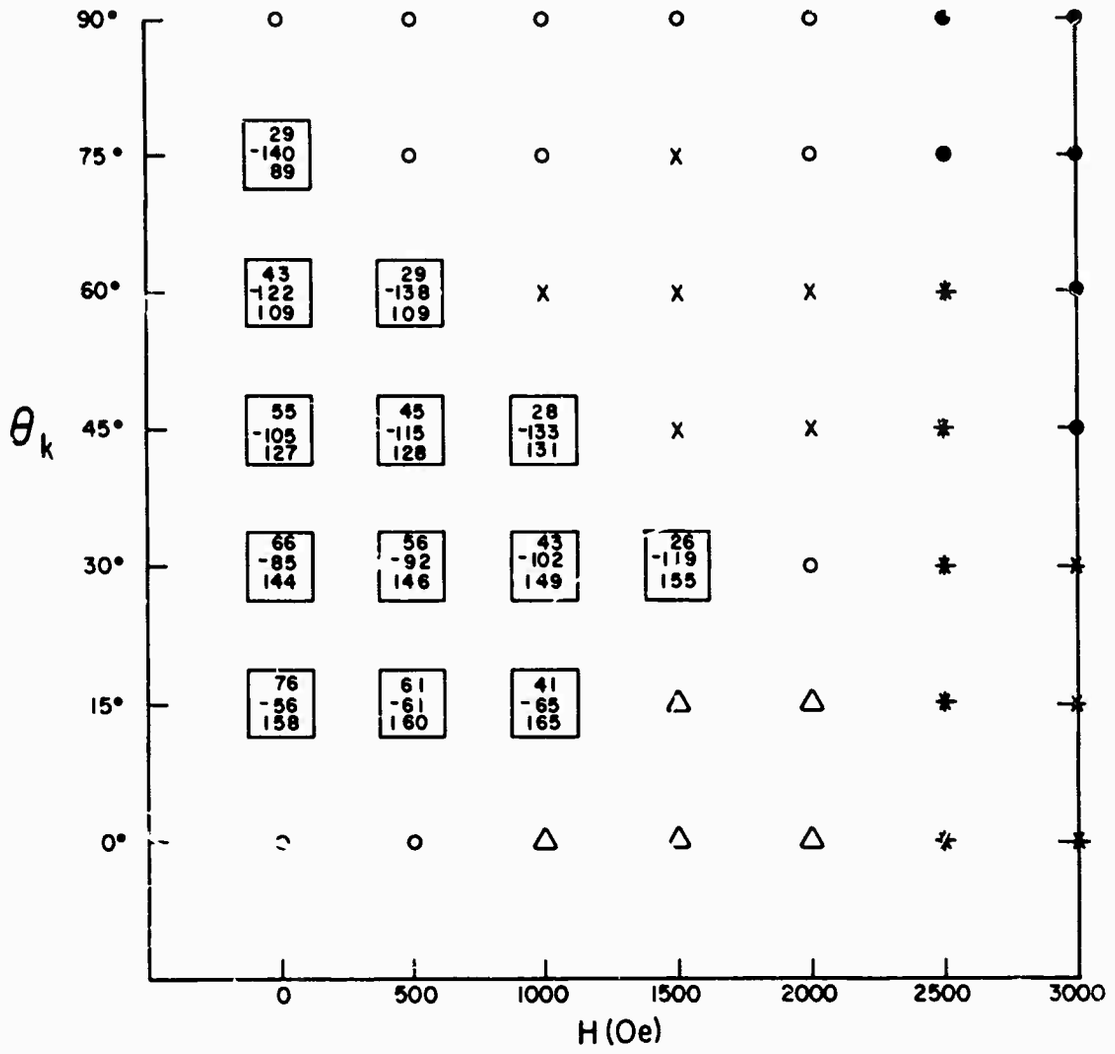

FIG. 5 Same as Fig. 2, except $\omega_k = 6.0 \times 10^{10}$ rad/sec. Note region of solutions has considerably contracted. For $\omega_k = 6.5 \times 10^{10}$ rad/sec, only three solutions would be indicated.

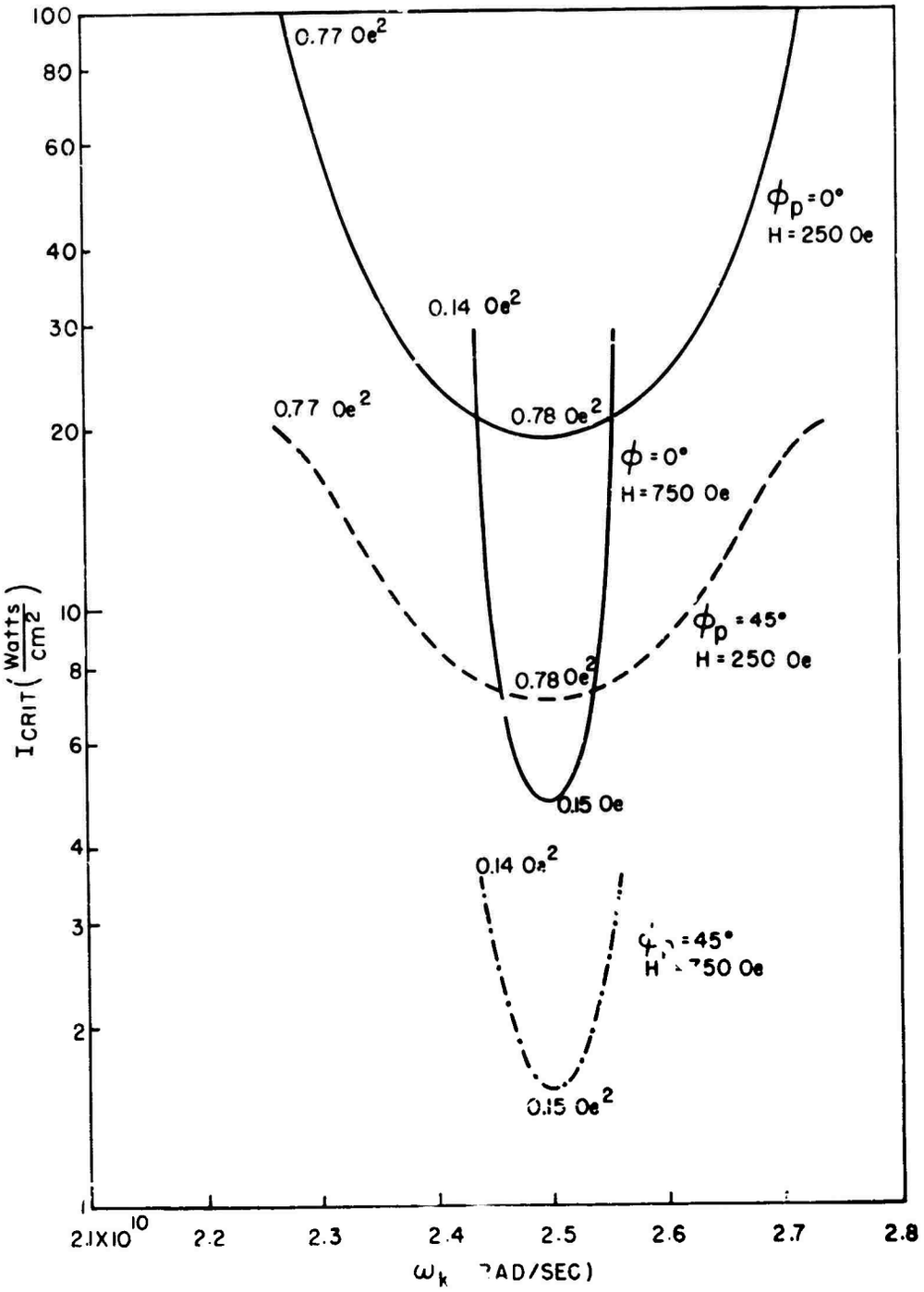

FIG. 6 Threshold acoustic intensity I_{CRIT} as a function of signal frequency ω_k, for a longitudinal pump of frequency 5×10^{10} rad/sec. The wave vectors $\tilde{k}_p$, $\tilde{k}$, and $\tilde{k}'$ lie in the xy-plane. The numbers lying along the curves give the product of spin-wave linewidths $\Delta H_k \Delta H_{k'}$ calculated according to formula (38) of the text.

The spin wave linewidths are functions of frequency and wave vector. We have used the simple formula[8]

$$\Delta H_k = a\omega_k + bk/\omega_k \quad , \tag{38}$$

with

$$a = 8.35 \times 10^{-18} \text{ gauss sec}$$

$$b = 5.24 \times 10^{4} \text{ gauss cm/sec}$$

in our numerical work.

In the case illustrated in Fig. 6, the variation with signal frequency of $\Delta H_k \Delta H_k$, is negligibly small. It does, however, vary with applied field and accounts for the lower minimum threshold at the higher field shown in the figure. Although the thresholds are not low for the cases illustrated in Fig. 6, the possible bandwidth is encouraging. For example, in the case of $\phi_p=45^0$, H=250 Oe, the threshold is within a factor of 2 of its minimum value over a band 7.5% on either side of $\omega_p/2$. This same case is shown again in Fig. 7, where we have also shown the variation in azimuthal angles ϕ_k, ϕ_k, as the signal frequency ω_k is varied. This variation, necessary for the conservation of wave vector and energy, is considerable for this case, namely about 80^0 over what would otherwise appear to be a useful band of frequencies.

Figure 8 shows the use of a transverse pump. Comparing to Fig 6, we see that the threshold is reduced by approximately a factor of 10 over a pump of longitudinal polarization. An unexpected feature of all the curves in Fig. 8 is the fact that the degenerate (in frequency) case has a maximum rather than a minimum threshold. This appears to be mostly a result of the variation of $\Delta H_k \Delta H_k$, which, at H=750 Oe, is markedly higher for the degenerate case.

Figure 9 shows the extremely broad bandwidth possible under operation with the signal wave vector inclined at 30^0 to the magnetic field H, rather than lying perpendicular to the field as does the pump wave vector. We have not shown the variation in signal azimuthal angle which

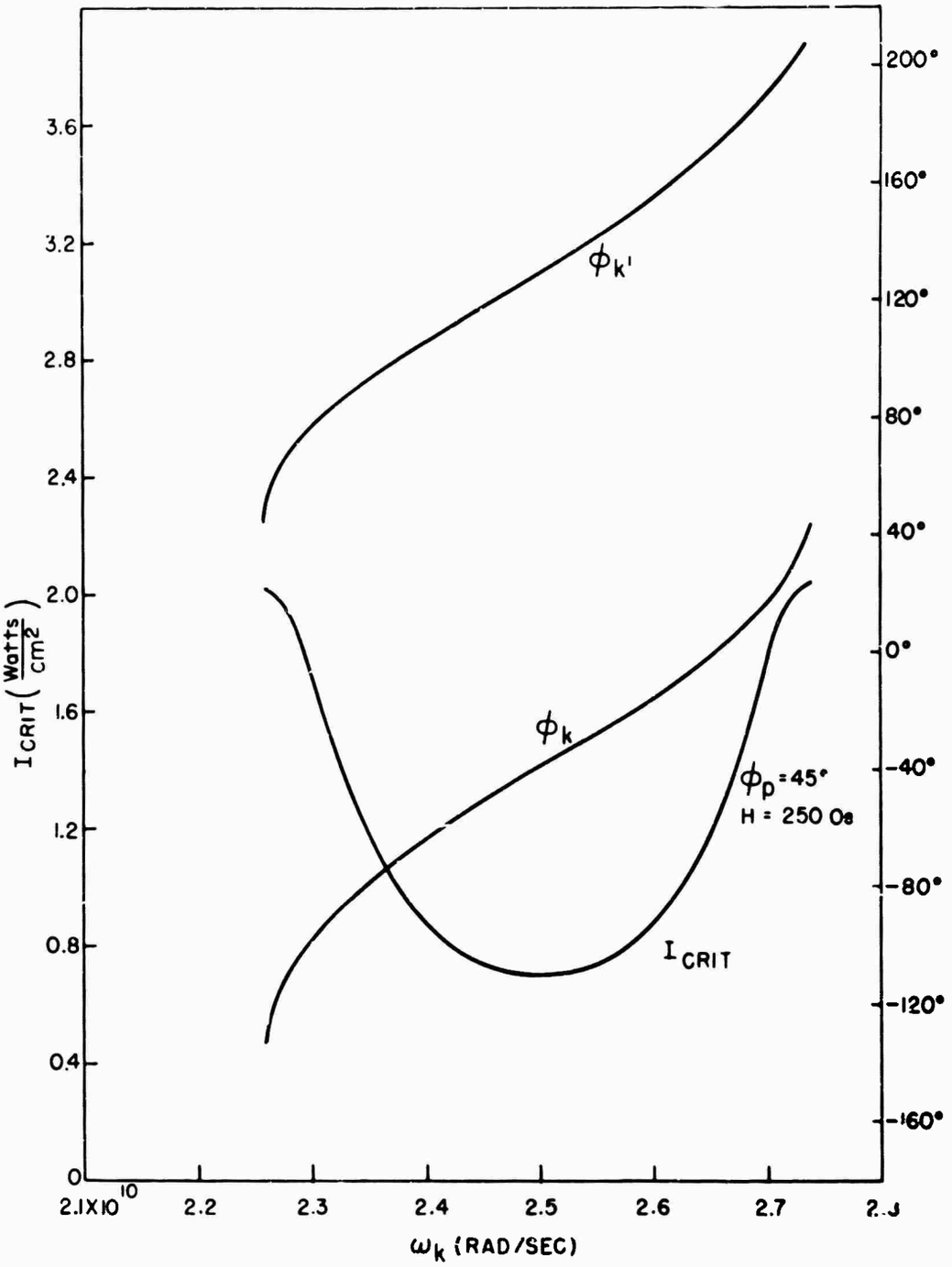

FIG. 7 Threshold acoustic intensity I_{CRIT}, and azimuthal angles for signal and idler wave vectors, as functions of signal frequency ω_k. The pump, of frequency 5×10^{10} rad/sec, is longitudinally polarized and all three wave vectors $\underset{\sim}{k}_p$, $\underset{\sim}{k}$, $\underset{\sim}{k}'$ lie in the xy-plane.

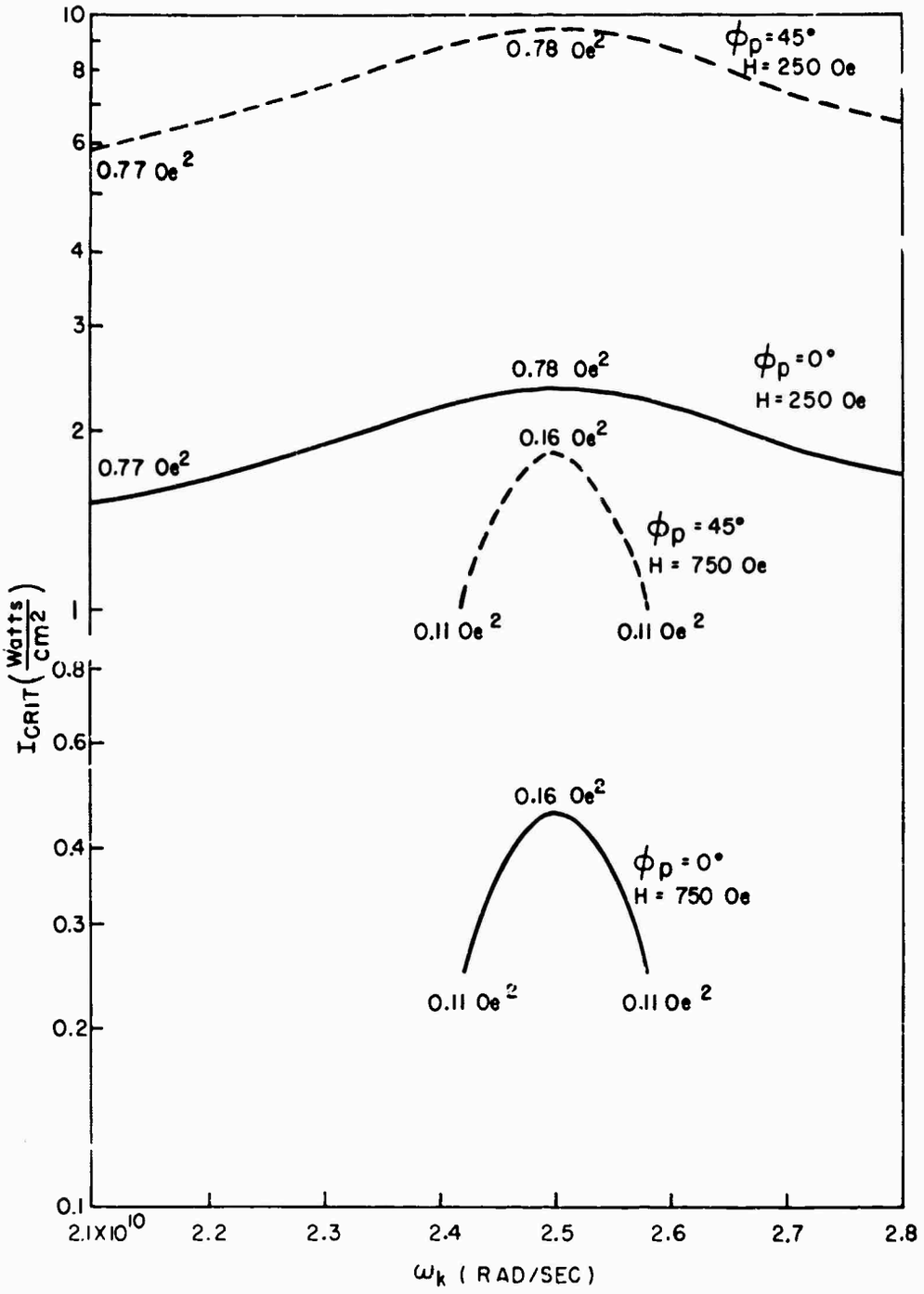

FIG. 8 Same as Fig. 6, except pump is transversely polarized along f´ .

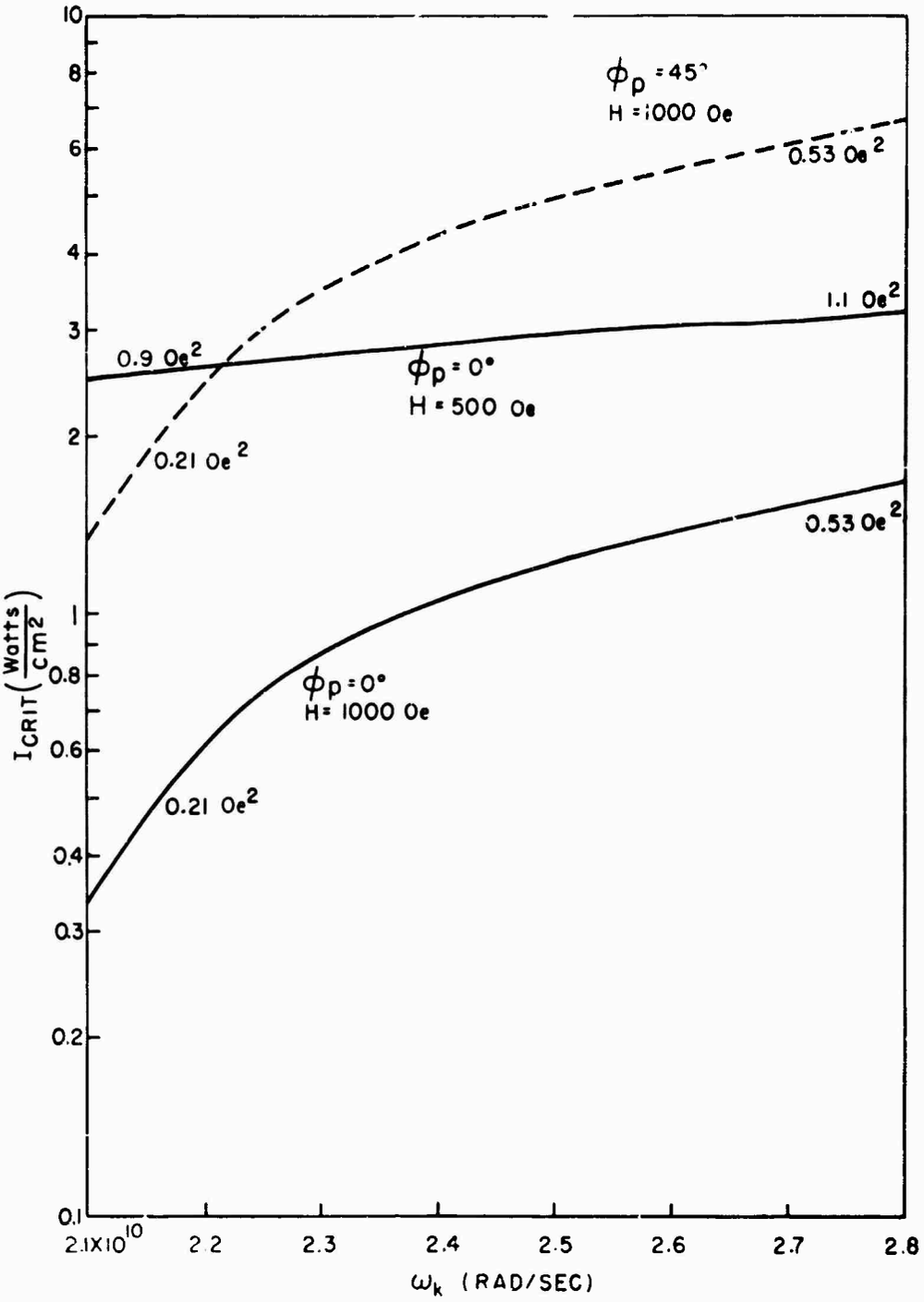

FIG. 9 Threshold acoustic intensity I_{CRIT} as a function of signal frequency ω_k, for a transverse pump of frequency 5×10^{10} rad/sec. The pump wave vector k_p lies in the xy-plane, with the magnetic signal wave-vector inclined $\sim 30^0$ to the magnetic field. The numbers lying along the curves give the product of spin-wave linewidths $\Delta H_k \Delta H_{k'}$ calculated according to formula (38) of the text.

the computation shows decreases from 71^0 to 23^0 as the frequency changes from 2.2×10^{10} rad/sec to 2.7×10^{10} rad/sec, for $\phi_p=0^0$, H=1000 Oe.

If the frequency is reduced, the threshold can drop markedly, as shown for example in Figs. 10 and 11. The pump frequency has been reduced from the previous cases by a factor of five. Again we see the phenomenon that for a transverse pump the threshold is highest for $\omega_k=\omega_p/2$. Although the bandwidth is rather small for the configuration shown in Fig. 10, the rather low threshold makes it a promising case for experimental study. In Fig. 11 we have shown the variation in azimuthal angles, which again is quite pronounced.

Figure 12 illustrates, at the lower frequency, the case of signal wave vector inclined at 30^0 to the magnetic field and again shows the wide bandwidth available under these conditions. The variations in signal and idler wave vector azimuthal angles ϕ_k and ϕ_k, and the variation of the polar angle θ_k, of the idler wave vector are shown in Fig. 13. In contrast to the other examples discussed, these variations are not large. In particular, the variation in ϕ_k is less than 1^0 over the 10% band illustrated in the figure.

The final figures (Figs. 14 and 15) are results for a longitudinal pump at the lower frequency and show features similar to those discussed above.

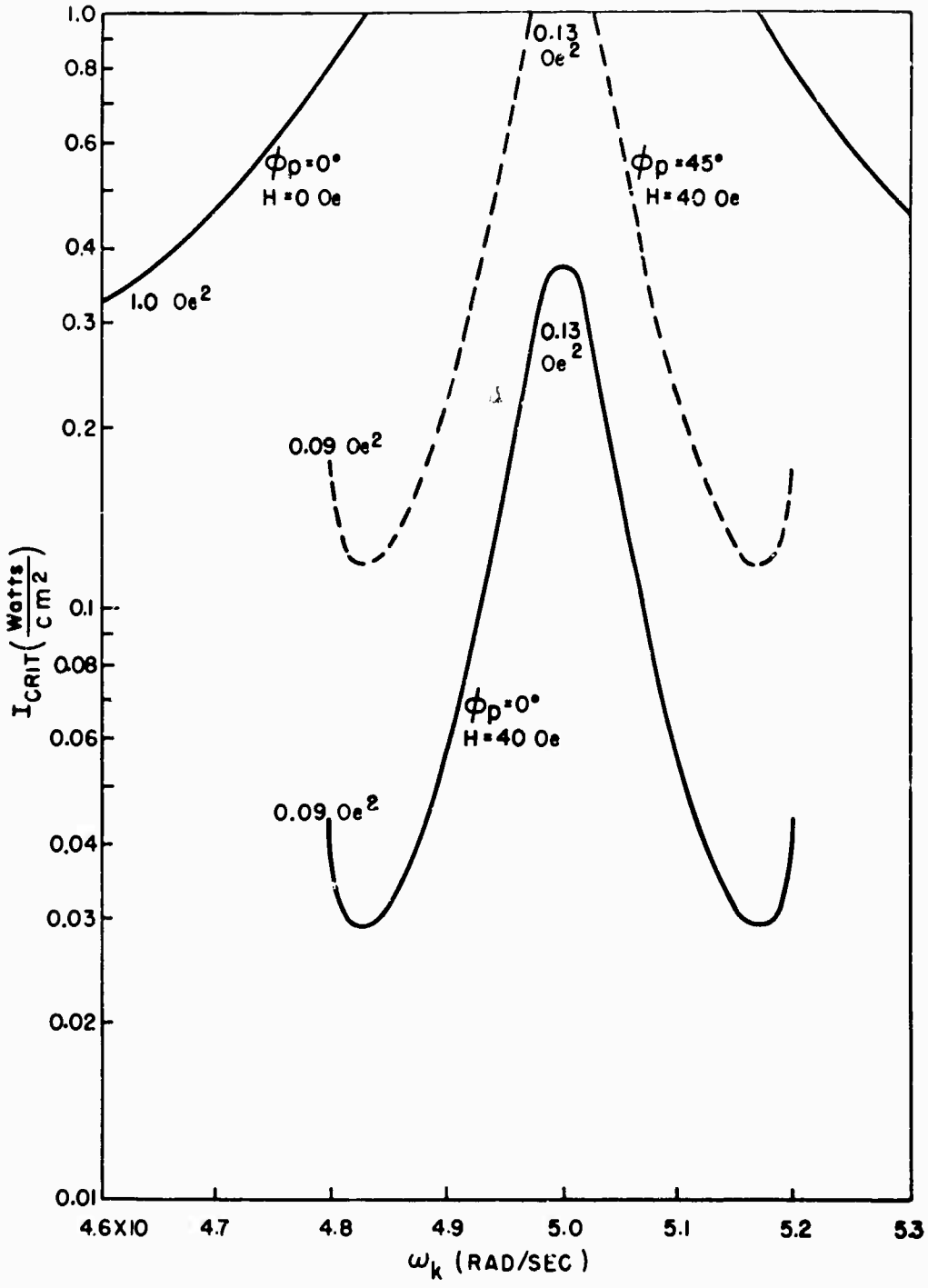

FIG. 10 Threshold acoustic intensity I_{CRIT} as a function of signal frequency ω_k, for a transverse pump polarized along $\hat{t}'$, of frequency 1×10^{10} rad/sec. The wave vectors k_p, k, and k' lie in the xy-plane. The numbers lying along the curves give the product $\Delta H_k \Delta H_{k'}$ calculated according to formula (38).

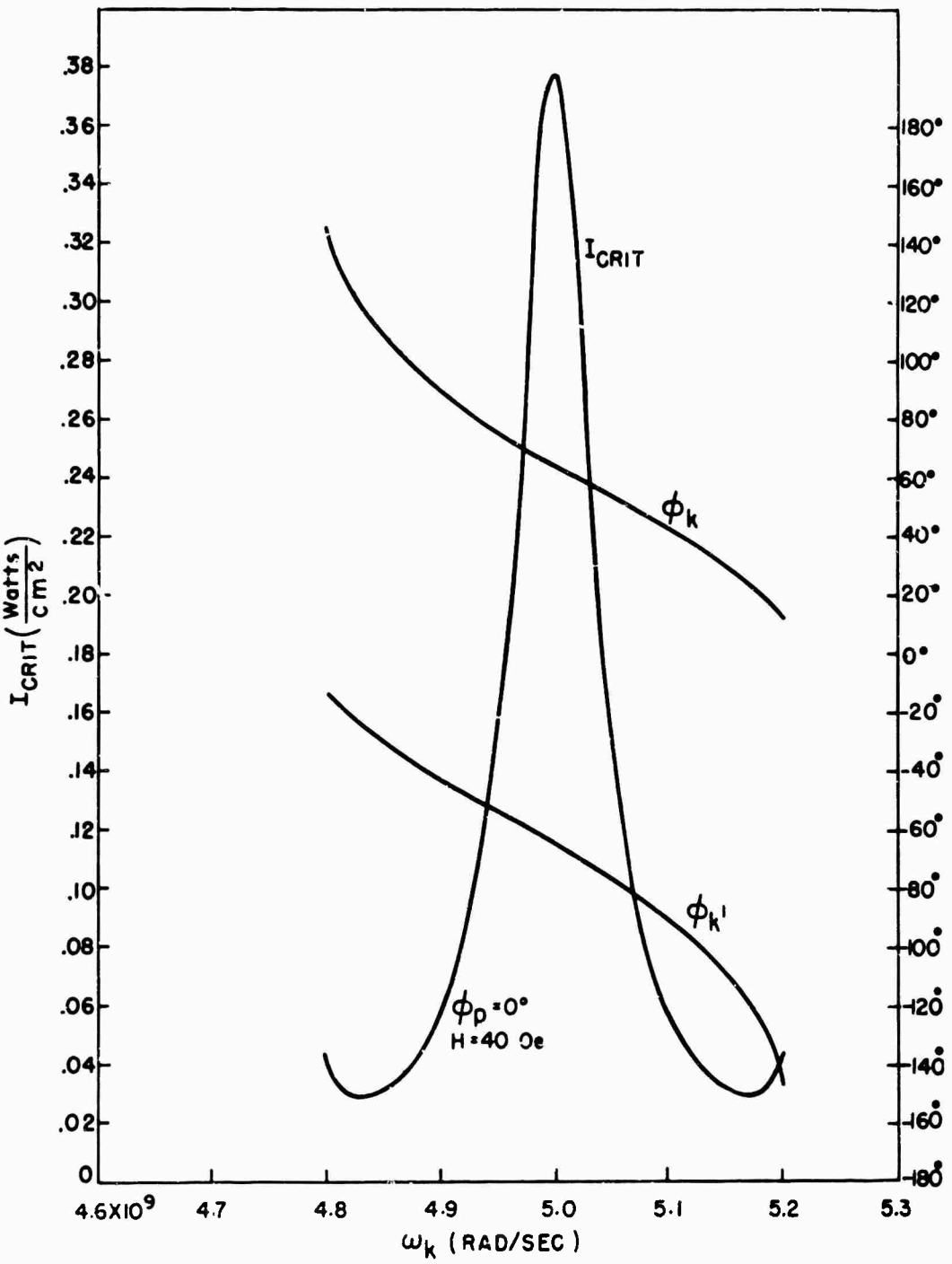

FIG. 11 Threshold acoustic intensity I_{CRIT}, and azimuthal angles for signal and idler wave vectors, as functions of signal frequency ω_k. The pump wave vector lies along x, and is transversely polarized along y. The pump frequency is 1×10^{10} rad/sec. All three wave vectors $\underset{\sim}{k}_p$, $\underset{\sim}{k}$, $\underset{\sim}{k}'$ lie in the xy-plane.

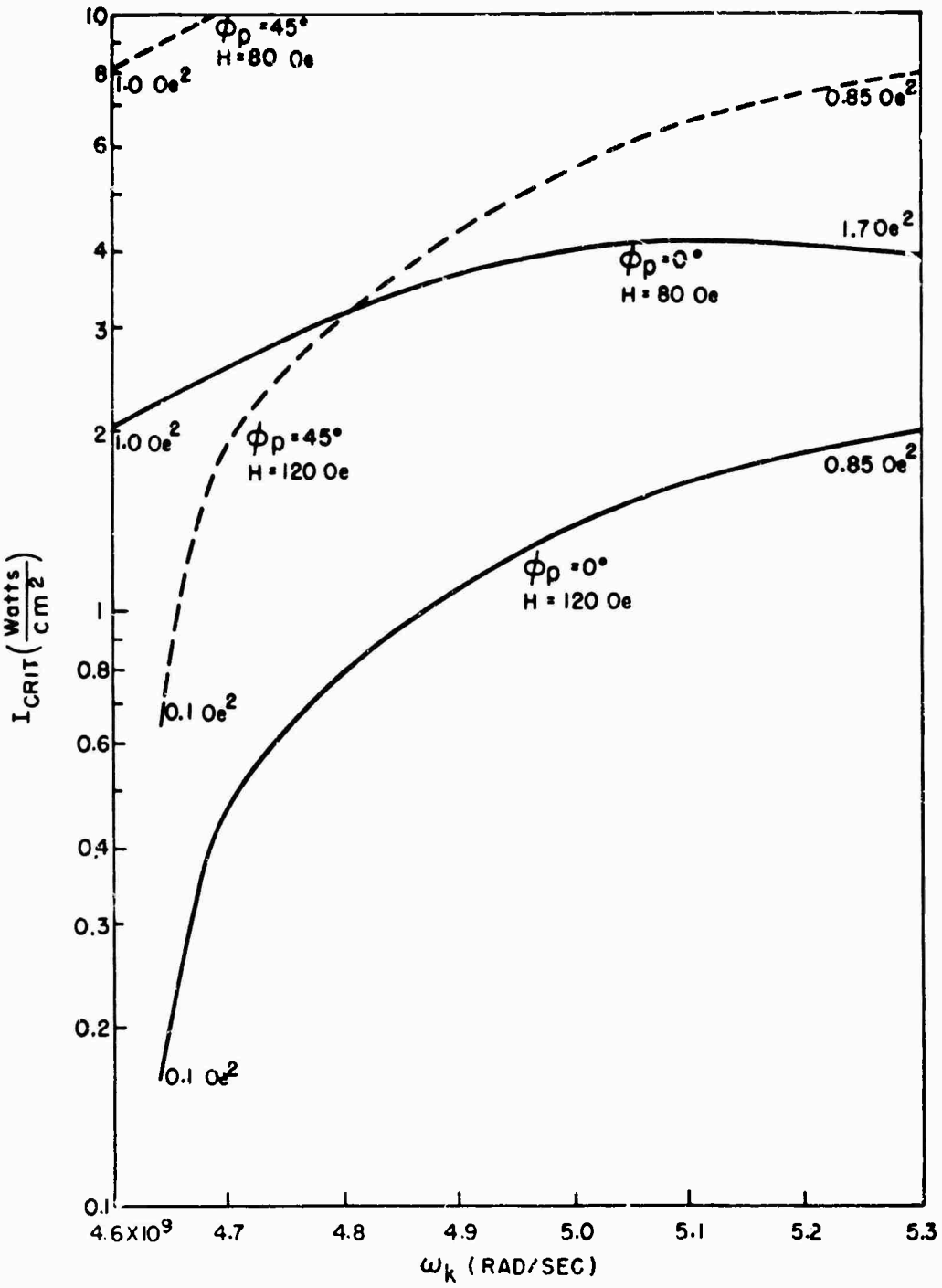

FIG. 12 Threshold acoustic intensity I_{CRIT} for a transverse pump polarized along $\hat{f}'$, of frequency 1×10^{10} rad/sec, with wave vector in the xy-plane. The signal wave vector is inclined at 30^0 to the magnetic field. The numbers lying along the curves give $\Delta H_k \Delta H_{k'}$.

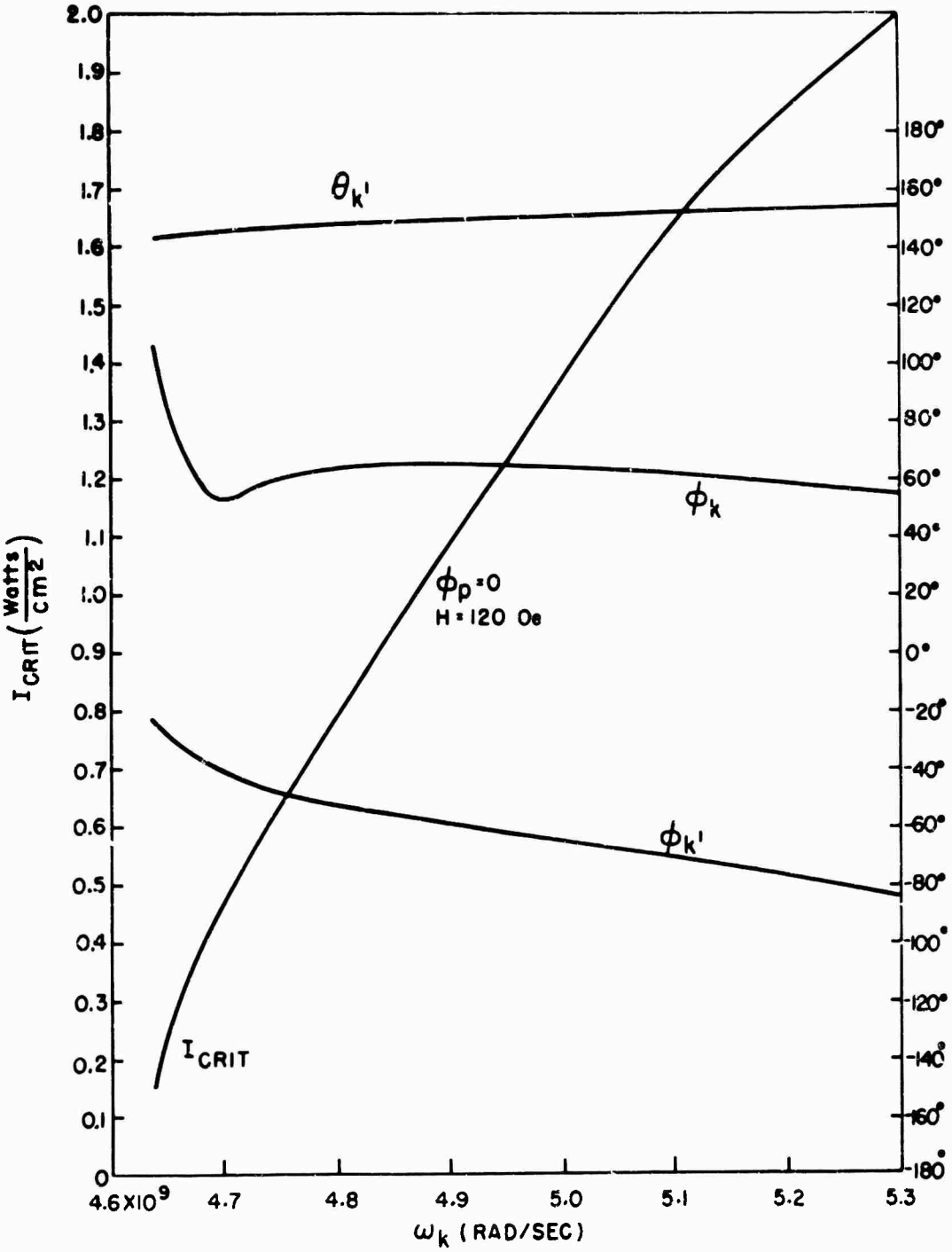

FIG. 13 Threshold acoustic intensity I_{CRIT}, azimuthal angles ϕ_k and $\phi_{k'}$ of the signal and idler wave vectors, and polar angle $\theta_{k'}$ of the idler wave vector as functions of the signal frequency ω_k. The pump, of frequency 1×10^{10} rad/sec, is transversely polarized along y, with the pump wave vector along x. The signal wave vector is inclined 30^0 to the magnetic field along z.

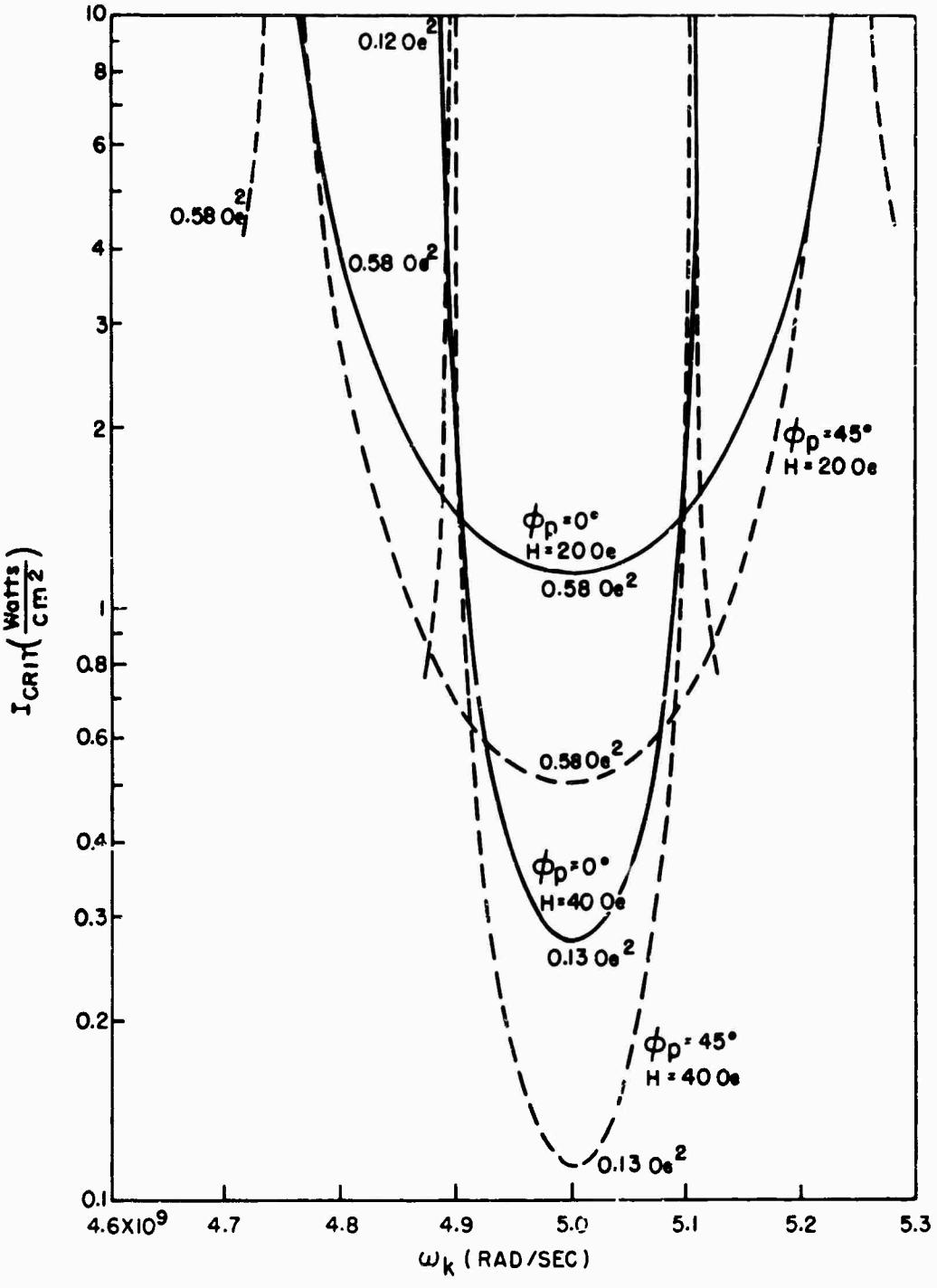

FIG. 14 Same as Fig. 6, except pump frequency is $\omega_p = 10^{10}$ rad/sec.

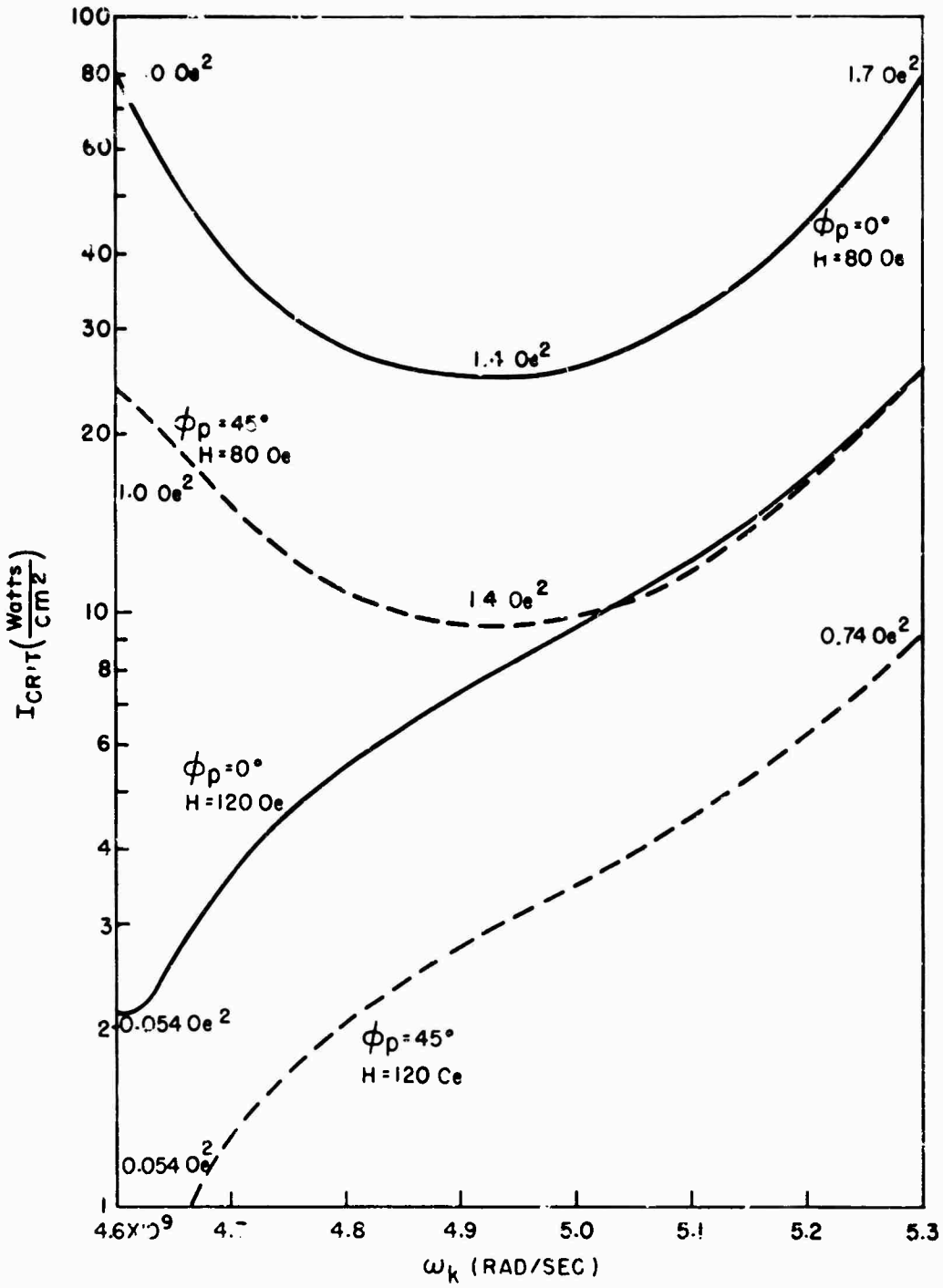

FIG. 15 Threshold acoustic intensity I_{CRIT} as a function of signal frequency ω_k, for a longitudinal pump of frequency 10^{10} rad/sec. The wave vector k_p lies in the xy-plane perpendicular to the internal field H. The signal wave vector is inclined 30^0 to H. The numbers lying along the curves give the product of spin-wave linewidths $\Delta H_k \Delta H_{k'}$ calculated according to formula (38) of the text.

SECTION III

EXPERIMENTS ON PARAMETRIC AMPLIFICATION OF SPIN WAVES BY TRAVELING PHONON PUMP

3.1 Transducers

Several techniques for establishing microwave phonon propagation in YIG are available. The magnetic techniques are not useful in the present studies. Among the piezoelectric techniques, thin film transducers are most efficient, and most likely to be improved. The cadmium sulphide thin film transducers used in the present development study were fabricated with the method described by Foster.[9]

These transducers may be excited in a transverse wave mode by an electric field normal to the film plane. At low frequencies (< 1.5 GHz) the film thickness is a half wavelength for transverse waves in the film. Good discrimination against longitudinal wave excitation (greater than 30 dB) can be obtained. However, as the frequency is increased, discrimination is degraded. To obtain good suppression of longitudinal excitation at frequencies greater than 1.5 GHz, it is possible to take advantage of the fact that the ratio of longitudinal to transverse phonon velocity in CdS is approximately 2.5:1. Thus a CdS film 5/2 transverse wavelengths thick will be one longitudinal wavelength thick, and longitudinal excitation is effectively suppressed. However, suppression of longitudinal wave excitation is obtained at the expense of transverse wave excitation efficiency since these are generated by an overtone mode.

Thin film CdS transducers are damaged when subjected to excessively high electric fields. In order therefore to obtain phonon power densities equal to or greater than the minimum required for spin wave excitation, transducers with adequate conversion efficiency are necessary. The theory of Sec. II indicates that phonon power densities of the order of 100 mW/cm^2 are required for the more favorable cases. (Note for instance Fig. 10.) In phonon pumping experiments it is convenient for a variety of reasons to use circuit matching structures with a Q of about 200 to drive transducers with an active area of approximately 0.1 cm^2. Our experience with

this configuration indicates that incident electromagnetic power in excess of 1 watt will damage the transducer. A trivial calculation shows that a total matching structure plus transducer conversion efficiency of about 1% is necessary to achieve phonon pumping. At the present state of the art this requirement can be met for frequencies up to 3 GHz.

Figure 16 is a schematic representation of a typical matching structure – transducer assembly.

3.2 Material

A single crystal ferrimagnetic material suitable for use in a phonon pumped magnetoelastic amplifier must have adequate magnetoelastic coupling and large elastic Q. YIG has these characteristics at room temperature for frequencies of 3 GHz or less. In order to avoid excessive pump power requirements a suitable material must also have a small spin wave linewidth ΔH_k.

Comparison of Fig. 10 with Fig. 12 shows that $\theta=\pi/2$ spin waves have the lowest instability threshold. The following discussion refers to such waves. ΔH_k, a function of frequency, has a minimum at 3 GHz increasing rapidly at lower frequencies in YIG.[10] We noted in Sec. 3.1 that transducer restrictions presently limit phonon pump frequencies to 3 GHz or less. This implies that any pair of potentially unstable spin waves also have frequencies less than 3 GHz and hence a large ΔH_k in YIG.

The increase of ΔH_k below 3 GHz is due to the presence of relaxation mechanisms not allowed at higher frequencies, the three magnon splitting processes. In these processes a spin wave with frequency ω_0 decays into two spin waves of lower frequency. One of these must have frequency $\omega<\omega_0/2$. Splitting processes are allowed at frequencies less than 3 GHz in YIG since the bottom of the spin wave band extends to frequencies less than 1.5 GHz when the top is at 3 GHz.

The width of the spin wave band depends on saturation magnetization M_s and the splitting processes are restricted to frequencies lower than 3 GHz in the gallium substituted isomorphs of YIG, $Y_3Ga_xFe_{5-x}O_{12}$, which have smaller M_s.

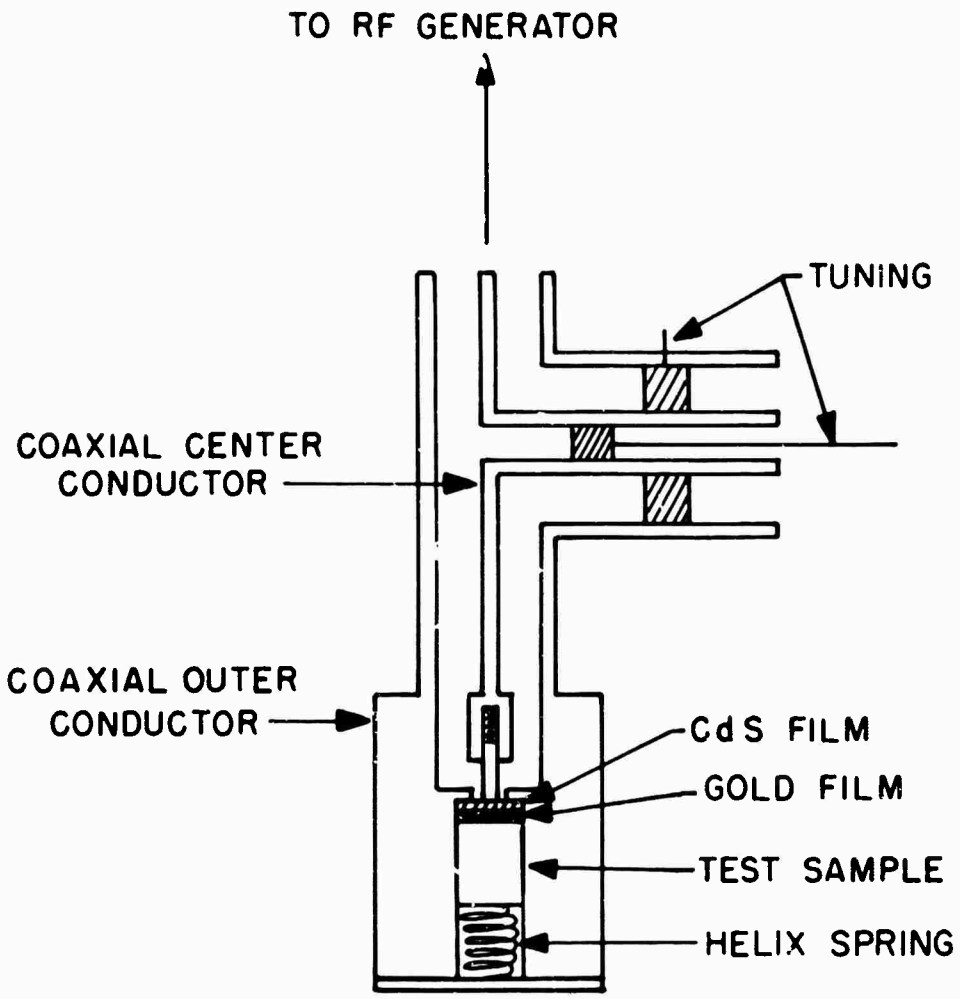

FIG. 16 Typical phonon generation assembly showing matching structure, CdS thin film transducer and test sample.

Single crystals of Ga-YIG with $4\pi M_s \approx 300$ are readily available from commercial sources and the phonon pumping experiment to be described later was made with such a crystal. Pertinent material parameters are exhibited in Table I, which also permits comparison with YIG.

Table I. Pertinent material parameters at 300^0K of YIG and Ga-YIG Crystal M380

	$4\pi M$ (gauss)	γ (MHz/Oe)	T_c (^{0}C)	$2K_1/M_s$ (Oe)	b_2 (ergs/cm^3)	Q_e (@ 3 GHz)
YIG	1750	2.80	287	90	7×10^6	12,500
M380	294	2.80	125	135	4×10^6	12,500

Note from Table I that $(M_s/b_2)_{YIG} = 3.3\ (M_s/b_2)_{M380}$. The theory of Sec. II shows that threshold strain is proportional to M_s/b_2. Thus, if other factors are equal, it takes less phonon power to parametrically excite spin waves in Ga-YIG than in YIG.

The influence of the magnetocrystalline anisotropy field $2K_1/M_s$ warrants discussion. The theory of Sec. II assumes $2K_1/M_s = 0$. This is a fairly good assumption for YIG and for high pump frequencies. Moreover the theory becomes considerably more complicated when the influence of $2K_1/M_s$ is treated exactly. Unfortunately, assuming $2K_1/M_s = 0$ is a poor assumption for M380 at the pump frequencies used in our experiments.

3.3 Pumping Experiments

3.3.1 Setup and procedure

The goal of the experimental development work was construction of a magnetoelastic amplifier and proceeded in two phases. The first phase consisted of observation of phonon pumping, the second of an attempt to realize an amplifying structure.

A block diagram of the setup used to observe phonon pumping is given in Fig. 17, which also exhibits the directions of the pertinent field vectors relative to crystal geometry.

CW microwave power from the traveling wave tube is converted to pulses of several microsecond duration at a convenient repetition rate. The electromagnetic energy is converted to phonon energy by the CdS transducer. Phonon pulses travel the length of the crystal, are reflected by the polished end face, return to the CdS transducer, and are converted to electromagnetic pulses. These are detected by the superheterodyne receiver and displayed on the oscilloscope. A typical display is shown in Fig. 18 which was chosen to show the effect of phonon pumping. When pumping occurs energy is delivered from the phonon pump to the excited spin waves. This is indicated by the reduced amplitude of the trailing edge of the pump pulse. Energy is extracted during the first round trip in the crystal. Subsequent echoes are replicas of the first reduced in amplitude by ordinary elastic loss mechanisms

The onset of pumping can be detected by observing the variation of pulse amplitude with increasing input power. The bias field is held constant at a value for which pumping is allowed. The onset of pumping becomes first noticeable as a decrease in amplitude at the trailing edge of the pulse. The power required for onset of pumping increases with decreasing pulse length. This dependence, due to the finite time required for excited spin waves to grow from their thermal amplitudes, is encountered in pulsed parallel pumping experiments and has been analyzed in detail.[11] Let $A(\tau)$ denote threshold pump amplitude for a pulse of duration τ. The analysis shows that $A(\tau)-A_{crit} \propto 1/\tau$, in which A_{crit} denotes threshold pump amplitude for cw pumping. Typical results from our experiments are shown in Fig. 19. The value of A_{crit} obtained by extrapolation should correspond to the amplitude calculated from a cw theory like that discussed in Sec. II.

Variation of the bias field alters the frequency and wave vector of the spin wave pairs that satisfy the conservation conditions, and since different pairs have different thresholds A_{crit} is a function of bias field H.

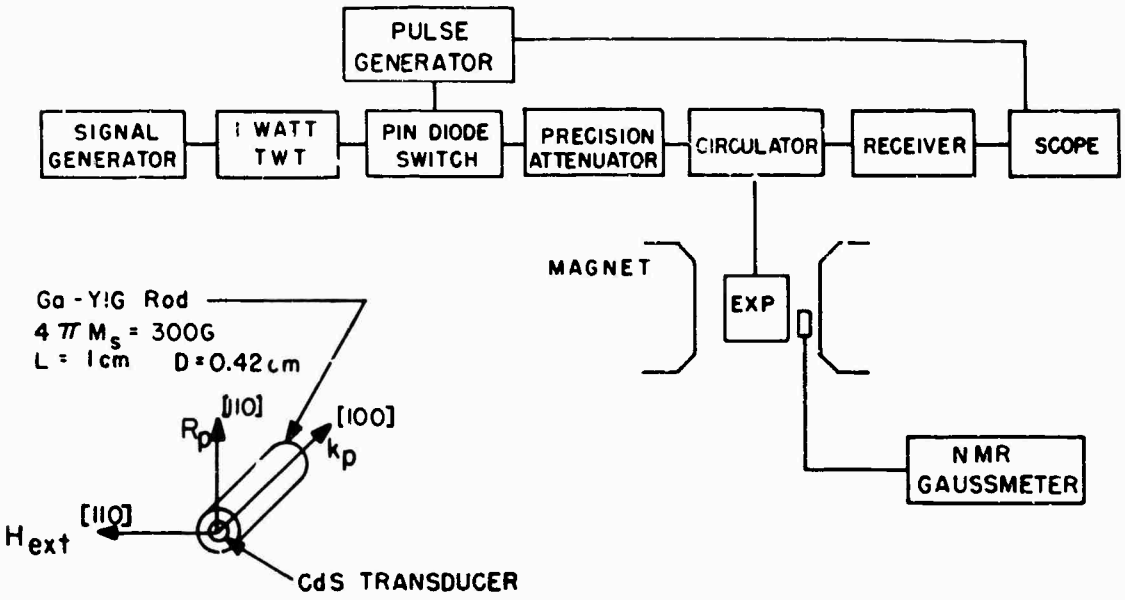

k_p Phonon propagation direction

R_p Direction of linearly polarized elastic displacement

H_{ext} Direction of bias magnetic field

FIG. 17 Experimental arrangement for observing phonon pumped spin wave instabilities.

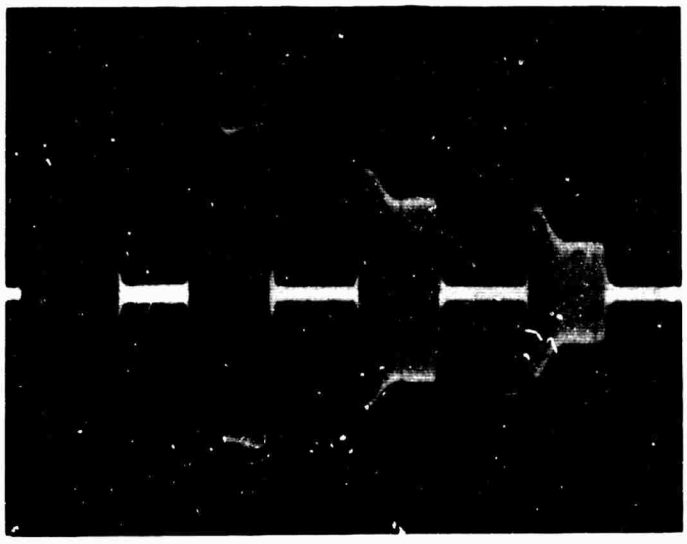

FIG. 18 Detected echoes of 2.4 GHz transverse phonon pulse. H_{ext} = 385 Oe. Approximately 0.5 watt incident on matching structure.

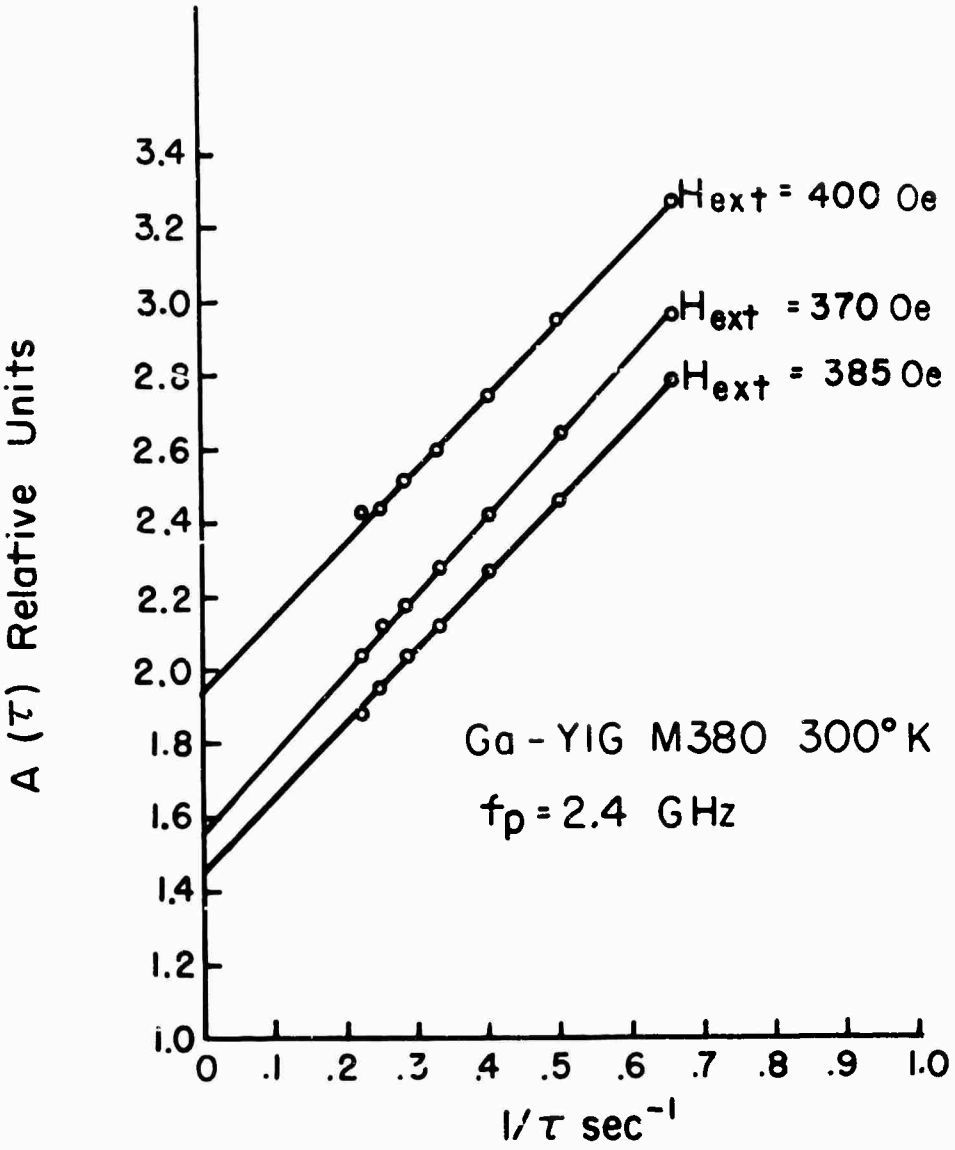

FIG. 19 Pump threshold amplitude, $A(\tau)$, as a function of reciprocal pulse length for several values of external magnetic field. Sample Ga-YIG M380. Pump frequency 2.4 GHz.

3.3.2 Results

Figure 20 exhibits A_{crit} vs H for the configuration shown in Fig. 17. The pump frequency was 2.4 GHz. Threshold amplitude is plotted as a function of external field H_{ext}.

The threshold minimum for H_{ext} = 385 Oe was expected. The internal field H_i in a uniformly, transversely magnetized rod varies symmetrically about the central cross section, being larger at the ends than at the center. H_i is relatively constant over only the central region, where H_i = 250 Oe for Ga-YIG M380 when H_{ext} = 385 Oe. For H_i = 250 Oe, the frequency of small k ($Dk^2 \ll H_i$), $\theta = \pi/2$ spin waves is approximately 1.2 GHz, half the 2.4 GHz pump frequency. Small k, $\theta = \pi/2$ spin waves have the lowest threshold. (Compare Fig. 10 and Fig. 12.) Thus when H_{ext} = 385 Oe the lowest threshold spin waves can be excited in the central region of the rod.

The increase in threshold for $H_{ext} > 385$ Oe was also expected. In this case $H_i > 250$ Oe in all regions of the rod, and at least one partner of any potentially unstable pair must have $\theta < \pi/2$ and a higher threshold than a $\theta = \pi/2$ pair.

The relatively slow increase in threshold for $H_{ext} < 385$ Oe is interesting. When $H_{ext} < 385$ Oe, $H_i < 250$ Oe in the central region of the rod. $\theta = \pi/2$ pairs are allowed, but at least one partner must have large k and large ΔH_k. Thus low threshold excitation is not expected in the central region. For 310 Oe $< H_{ext} <$ 385 Oe a low threshold $\theta = \pi/2$ spin wave pair can be excited in some region Δz, between the center and ends, in which $H_i = 250 \pm \epsilon$ Oe. Such a pair would move toward the center, lower field region with an attendant increase in k and ΔH_k ending parametric growth perhaps in a time short compared to the time required to grow to detectable amplitude. Thus low threshold excitation in the end regions of the rod might not be expected.

The relatively slow increase of A_{crit} as H_{ext} is decreased could result if both partners of a $\theta = \pi/2$ pair excited in Δz had sufficiently small group velocity to remain in Δz for a time long compared to pump pulse duration. As H_{ext} is lowered, Δz would move from the rod center, getting

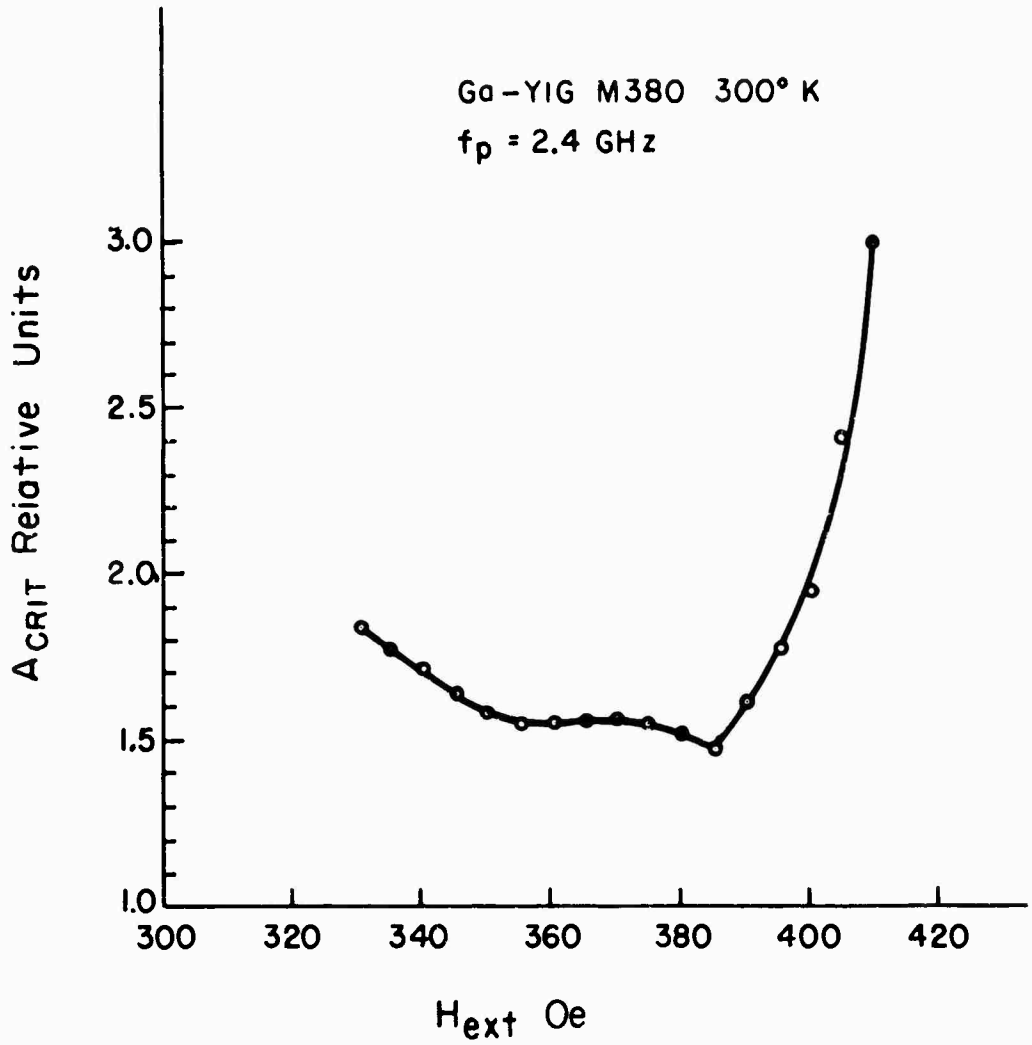

FIG. 20 Pump threshold amplitude, A_{crit} , as a function of external magnetic field. Sample Ga-YIG M380. Pump frequency of 2.4 GHz.

narrower as it approached the rod end. As the volume of active region is reduced, the total energy extracted from the pump pulse would also be reduced. This mechanism would account for the relatively slow increase of A_{crit} for $H_{ext} < 385$ Oe.

SECTION IV

AMPLIFICATION EXPERIMENTS

4.1 Amplifier Design

The amplifier structure depicted schematically in Fig. 21 was suggested by the results of the pumping experiments, and by the reasonably well understood mechanisms of magnetoelastic wave generation and propagation in axially magnetized YIG rods.[12] The magnetic fields associated with a pulsed rf current in a fine wire generate a spin disturbance, probably a traveling magnetostatic mode, that excites a $\theta=0$ spin wave in a region Δz in the rod where $f \approx \gamma H_i$. The spin wave travels toward the rod end in the direction of decreasing field, soon being converted to an elastic wave which travels to the polished end of the rod and is reflected. The sequence is then reversed, resulting finally in a pulse of rf current in the wire. Similar experiments have been tried in transversely magnetized YIG rods with limited success. In a transversely magnetized rod a $\theta=\pi/2$ spin wave excited in a region Δz where $f \approx \gamma\sqrt{BH_i}$ would travel toward the rod center and be converted to an elastic wave. The elastic wave would travel through the rod center to the symmetric region where $f \approx \gamma\sqrt{BH_i}$, be reconverted to a spin wave and reflected back for detection. It was envisioned that the spin wave could be parametrically amplified by a transverse phonon pump either at the region of excitation or reflection.

The limited success in generating, propagating, and detecting spin waves in transversely magnetized rods has been experienced using YIG. It was felt that the lower $4\pi M_s$ of Ga-YIG M380 increased the probability of successful operation, particularly for low frequency magnetoelastic waves.

4.2 Results

Operation of the amplifier was attempted using Ga-YIG M380. Although it was possible to excite magnetostatic modes in the transversely magnetized rod over a wide range of frequencies centered about 1.2 GHz none was amplified by a 2.4 GHz transverse phonon pump pulse.

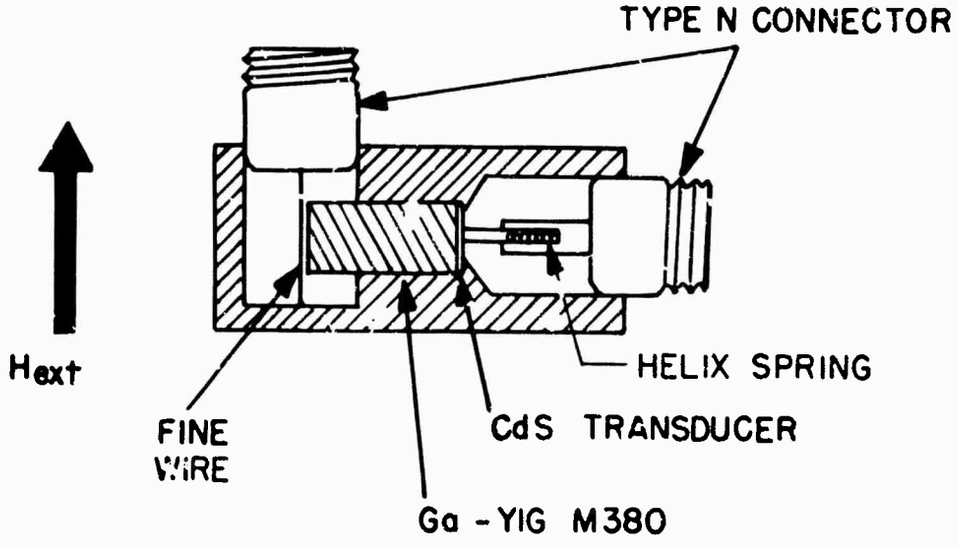

FIG. 21 Schematic of amplifier structure.

Excitation of a magnetoelastic wave pulse by means of the fine wire was attempted. No pulses were detected. Phonon pumping at 2.4 GHz was applied with sufficient power to observe energy loss from the pump. A wide range of frequencies centered about 2.2 GHz was searched. No signals were observed. Combinations of excitation and pumping were also attempted; these also failed to yield any signals.

SECTION V

CONCLUSIONS AND SUGGESTIONS FOR FURTHER DEVELOPMENT WORK

Although this development program did not result in a magnetoelastic wave amplifier with usable bandwidth, the positive results of the program are encouraging. The theory shows that only moderate pump power is required to attain threshold and pump a wide variety of spin wave modes. The experimental work showed that presently available materials and transducers can be employed to achieve pumping at frequencies up to 3 GHz.

The failure of the amplifier device was probably due to the unfavorable configuration for nonparametric generation of a signal mode. Testing alternative configurations is a fruitful area for further development work. An attractive candidate is a disk with parallel flat spots polished at opposite ends of a diameter. This configuration is more difficult to fabricate than a rod, but more favorable for nonparametric generation of a signal mode.

SECTION VI

REFERENCES

1. B. A. Auld and H Matthews, J. Appl. Phys. 36, 3599 (1965).
2. H. Matthews, Phys. Rev. Letters 12, 325 (1964).
3. R. W. Damon and H. van de Vaart, Appl. Phys. Letters 6, 152 (1965).
4. R. W. Damon and H. van de Vaart, Appl. Phys. Letters 6, 194 (1965).
5. H. Matthews and F. R. Morgenthaler, Phys. Rev. Letters 13, 614 (1964).
6. W. Strauss, Proc. IEEE 53, 1485 (1965).
7. R. L. Comstock, Proc. IEEE 53, 1508 (1965).
8. See for instance, R. L. Comstock, Appl. Phys. Letters 6, 29 (1965).
9. N. F. Foster, Proc. IEEE 53, 1400 (1965).
10. See for instance, Marshall Sparks, Ferromagnetic Relaxation Theory (McGraw-Hill, N.Y., 1964).
11. U. Milano and E. Schlömann, Raytheon Technical Memorandum T-265 (1960).
12. R. W. Damon and H. van de Vaart, Proc. IEEE 53, 348 (1965).

UNCLASSIFIED
Security Classification

DOCUMENT CONTROL DATA - R&D

(Security classification of title, body of abstract and indexing annotation must be entered when the overall report is classified)

1. ORIGINATING ACTIVITY *(Corporate author)*
SPERRY RAND RESEARCH CENTER
under Purchase Order to M.I.T. Lincoln Laboratory

2a. REPORT SECURITY CLASSIFICATION
unclassified

2b. GROUP
none

3. REPORT TITLE
DEVELOPMENT PROGRAM ON MAGNETOELASTIC WAVE AMPLIFIER

4. DESCRIPTIVE NOTES *(Type of report and inclusive dates)*
Final Technical Report (30 June 1966 - 30 June 1967)

5. AUTHOR(S) *(Last name, first name, initial)*
Matthews, H. and Lyons, D. H.

6. REPORT DATE	7a. TOTAL NO. OF PAGES	7b. NO. OF REFS
OCTOBER 1967	51	12

8a. CONTRACT OR GRANT NO.	9a. ORIGINATOR'S REPORT NUMBER(S)
AF 19(628)-5167	SRRC-CR-67-51
b. PROJECT NO. ARPA Order 498	9b. OTHER REPORT NO(S) *(Any other numbers that may be assigned this report)* ESD-TR-67-573
c.	
d.	

10. AVAILABILITY/LIMITATION NOTICES
This document has been approved for public release and sale; its distribution is unlimited.

11. SUPPLEMENTARY NOTES	12. SPONSORING MILITARY ACTIVITY
none	Advanced Research Project Agency Department of Defense

13. ABSTRACT

A general theory of parametric excitation of spin waves by a traveling phonon in a ferromagnet is presented. The theory yields expressions for the minimum phonon intensity required for excitation of a pair of spin waves. For certain cases of practical interest the threshold expressions together with the conservation conditions for parametric amplification are used through a computer program to generate curves of the functional relation between pertinent variables. Experiments utilizing suitable transducers and ferrimagnetic material are described. These experiments extend observation of the basic phenomena to include phonon pumping by transverse waves. An amplifier device, of exploratory nature, was designed and tested.

14. KEY WORDS
Parametric Amplification
Spin Waves
Phonon Pumping

UNCLASSIFIED
Security Classification